



The Left and Right Ventricles

6

Francesco F. Faletra, Laura A. Leo, Vera L. Paiocchi,
Susanne A. Schlossbauer, Giovanni Pedrazzini,
Tiziano Moccetti, and Siew Yen Ho

As in the previous chapters, the three imaging techniques will be used to illustrate anatomy. In this chapter we describe the anatomy of left ventricle (LV) and right ventricle (RV).

The Left Ventricle

The Shape

The LV resembles an ellipsoid of revolution with its long axis directed from the base to the apex. All three noninvasive imaging techniques show this ellipsoidal geometry with cross-sections parallel to the long axis (meridian sections). Conversely, short axis cross-sections from the base to the apex reveal a circular geometry. Consequently, the interventricular septum is curved with the concavity toward the LV (Fig. 6.1). Differences also exist in the thickness of the musculature of the ventricular wall: in the normal individual the LV free wall is the thickest (12–14 mm) at the cardiac base and gradually decreases toward the apex. At the very tip of the apex the wall thickness is as thin as 2 mm (Fig. 6.2).

F. F. Faletra (✉) · L. A. Leo · V. L. Paiocchi · S. A. Schlossbauer
Non-invasive Cardiovascular Imaging Department, Fondazione
Cardiocentro Ticino, Lugano, Switzerland
e-mail: Francesco.Faletra@cardiocentro.org;
lauraanna.leo@cardiocentro.org; vera.paiocchi@cardiocentro.org;
susanne.schlossbauer@cardiocentro.org

G. Pedrazzini · T. Moccetti
Cardiology Department, Fondazione Cardiocentro Ticino,
Lugano, Switzerland
e-mail: giovanni.pedrazzini@cardiocentro.org;
tiziano.moccetti@cardiocentro.org

S. Y. Ho
Royal Brompton Hospital, Sydney Street, London, UK
e-mail: yen.ho@imperial.ac.uk

Inlet, Apical Trabeculated, and Outlet Components

The left ventricle can be divided empirically into an inlet, an apical trabeculated, and an outlet component, although well-demarcated anatomic boundaries between these three regions do not exist. Furthermore, trabeculations (muscle bundles) are not strictly limited to the apical component. Only the smooth wall of the upper part of the septum, beneath the aortic valve, is devoid of trabeculations, while the *inlet* component contains the mitral valve, chordae tendineae, and papillary muscles (PMs), and extends from the mitral hinge line to the attachment of papillary muscles. This component may present with a fairly smooth wall.

The *apical* component is characterized by fine trabeculations—thin muscular bundles that arise from compact myocardium. Not infrequently, finer strands known as false tendons extend from the septal surface, crossing the cavity to insert into the PMs and the free wall. The trabeculated component of LV roughly comprises one third of the LV but both extensions and lengths of the trabeculae into the LV cavity are highly variable among individuals.

Extensive trabeculations are, in fact, frequently found in healthy individuals. The presence of highly trabeculated LV, though, in the absence of any other structural heart disease, has raised concerns as to whether this is a pre-phenotypic marker of underlying structural heart disease such as myocardial non-compaction with potentially adverse outcome, or is just a normal anatomical variant. Studies with CT scan (the noninvasive imaging technique with highest spatial resolution power) have shown that extensive trabeculations reaching the criteria threshold for the diagnosis of non-compaction myocardium (i.e., transmural wall thickness of non-compaction to compact myocardium ratio > 2.3 in diastole) have been found also in normal healthy individuals (Fig. 6.3a, b). Moreover, studies with cardiac magnetic resonance have shown in asymptomatic individuals that marked extension of trabeculations in the

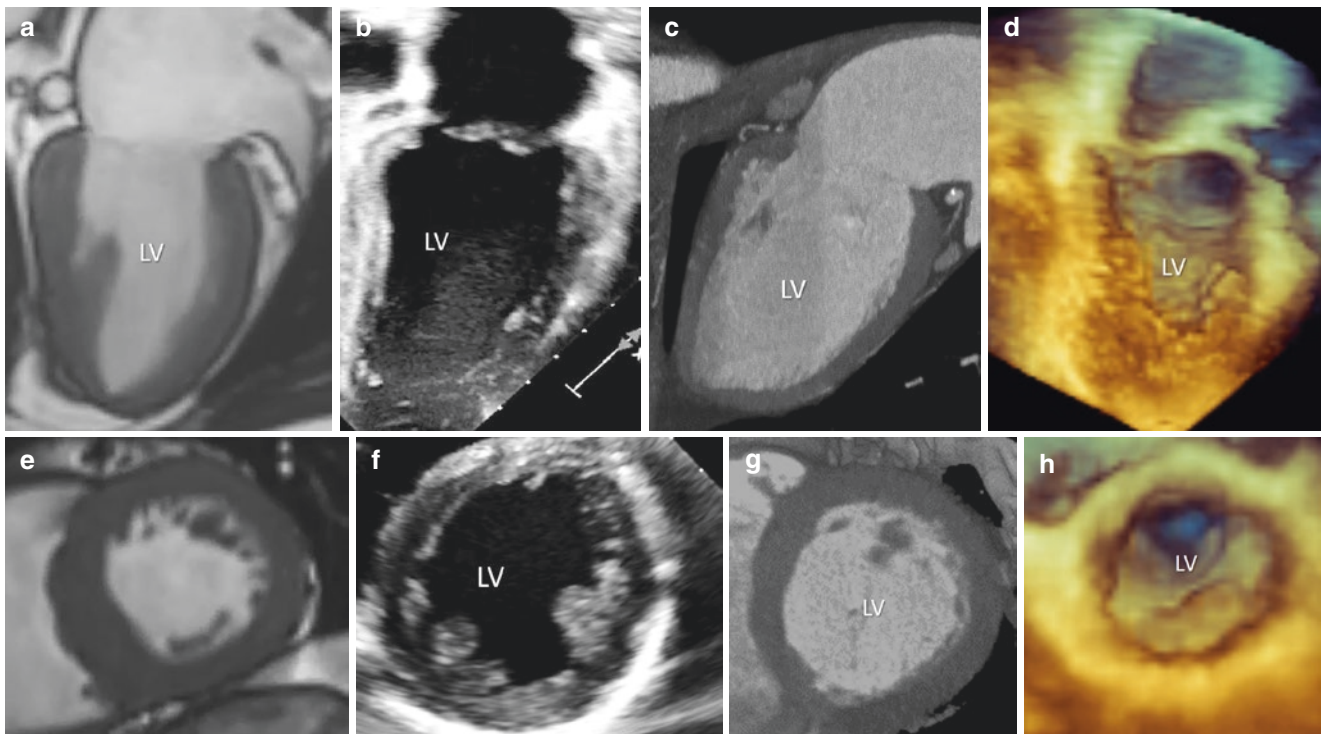


Fig. 6.1 Two-chamber long-axis views (**a–d**) and (**e–h**) short-axis view at mid-level obtained with cardiac magnetic resonance (**a–e**); 2D transthoracic echocardiography (**b–f**); computed tomography (**c, g**); and three-dimensional echocardiography (**d, h**). Showing as in long-

axis sections along the meridians (**a–d**), the LV has an ellipsoid-shaped configuration, while in short-axis cross sections (**e–h**), the LV assumes a circular configuration

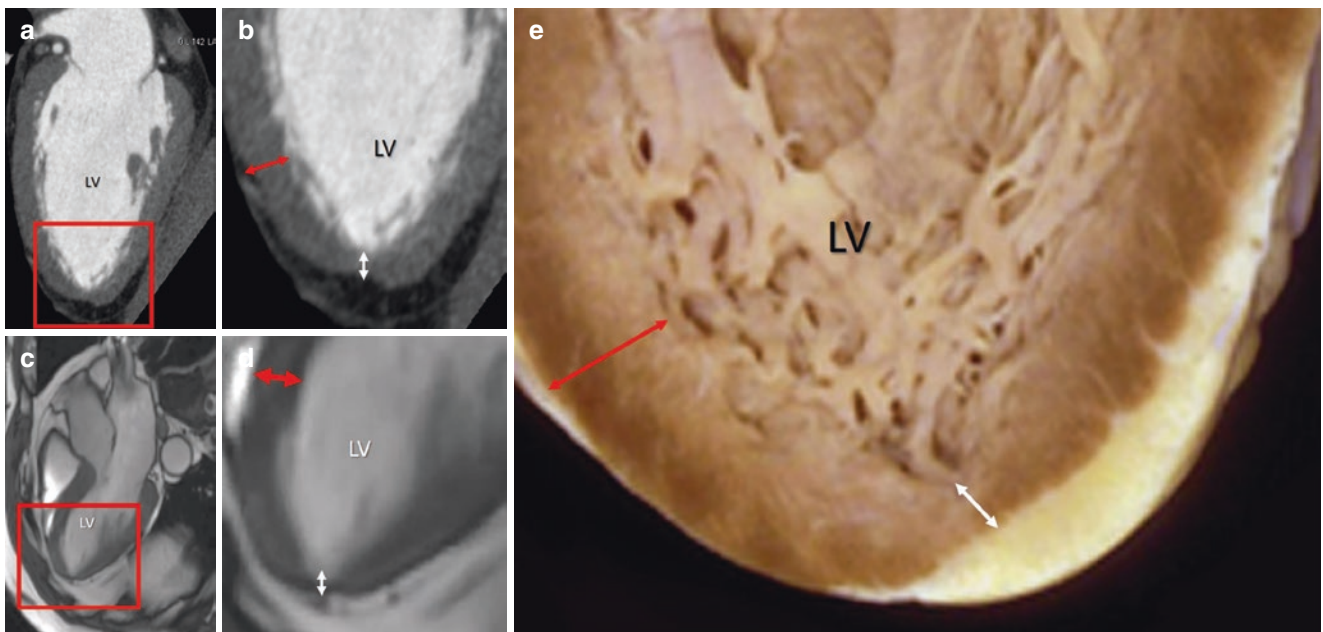


Fig. 6.2 (a) Computed tomography planar image in two-chamber view and (c) cardiac magnetic resonance in long-axis view. The areas in red boxes are magnified in (b) and (d) respectively. Both techniques beautifully visualized as the tip of apex is thinner (*white double arrow*) than

the anterior (*red double arrow* in **b**) or septal (*red double arrow* in **d**) left ventricle (LV) walls. (e) Anatomical specimen showing the differences in thickness between the apex (*white double arrow*) and the lateral wall (*red double arrow*)

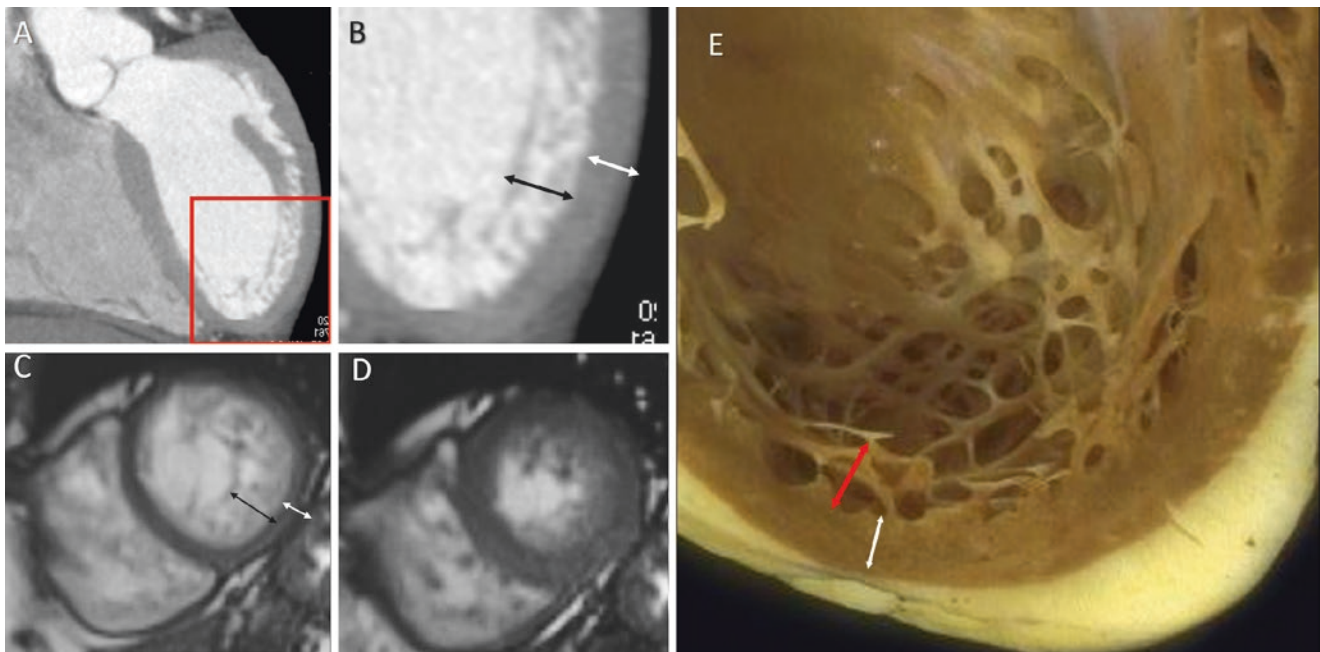


Fig. 6.3 (a and b) CT scan multiplanar imaging format in long axis view. The area in the red box is magnified in panel (b). Images show an extensive trabeculation in an otherwise normal individual. Black and white double-headed arrow illustrates the thickness of trabeculated and compact layers respectively (c, d). CMR cine image in short-axis view in diastole (c) and systole (d), showing an extensive trabeculation with

normal contractility. *Black and white double arrows* indicate the thickness of trabeculated and compact layers respectively. (e) Anatomic specimen showing a highly trabeculated left ventricle in an otherwise normal heart. *Red and white double arrows* indicate the thickness of trabeculated and compact layers respectively

absence of structural heart disease, at a follow-up of as long as 10 years, is not associated with a decline of systolic function or symptoms (i.e., heart failure, ventricular arrhythmias, and systemic embolic events) (Fig. 6.3c, d). Thus, subjects with marked trabeculations in absence of any other clinical pathological aspects should not be labelled as having a potential cardiomyopathy.

Particularly interesting is the presence of highly trabeculated myocardium in athletes. Although these findings have been considered as a nonspecific epiphenomenon in response to a chronic increase in preload and afterload associated with extreme exercise, a “gray zone” and concern still persist because more or less concealed cardiomyopathy is considered one of the most common causes of effort-related sudden death in young athletes. The dilemma in differentiating between “benign” and “malignant” hypertrabeculation is due to the “ambiguous” criteria used for the diagnosis of non-compaction myocardium. Indeed, although these criteria are based on the net distinction between an outer layer where the myocardium is compacted and an inner layer formed by trabeculations and deep recesses, this latter aspect is variable in extension and in site; thus the precise point in space and in time for measuring the thickness of the two layers is still uncertain. Additional criteria (such as inappropriate increase of LV volume, reduced ejection fraction or longitudinal LV short-

ening, abnormal diastolic function, ECG anomalies, and eventually reduction of exercise capability) should be taken into account to avoid diagnosing non-compaction myocardium based merely on imaging.

The *outlet* component sustains the aortic root, but contrary to the RV outlet, which is completely muscular, the LV outlet consists of both muscular and fibrous tissues. Indeed, the posterior-medial part of the LV outlet is formed by the zone of mitral aortic continuity. This is a band of fibrous tissue that connects the hinge-line of the anterior mitral leaflets with the inter-leaflet fibrous triangle between left and non-coronary sinuses and extends between the left and right fibrous trigones. A small area of the medial aspect of LV outlet is occupied by the membranous septum. The anterolateral aspect (almost half of the outlet circumference) is formed by musculature of ventricular septum and LV wall. Since the LV outlet component is also part of the aortic root, readers will find an additional description of the LV outlet in Chap. 2.

Papillary Muscles

Papillary muscles (PMs) are considered one of the distinctive aspects of the LV. There are usually two groups. Viewed from the atrial perspective, these two groups of

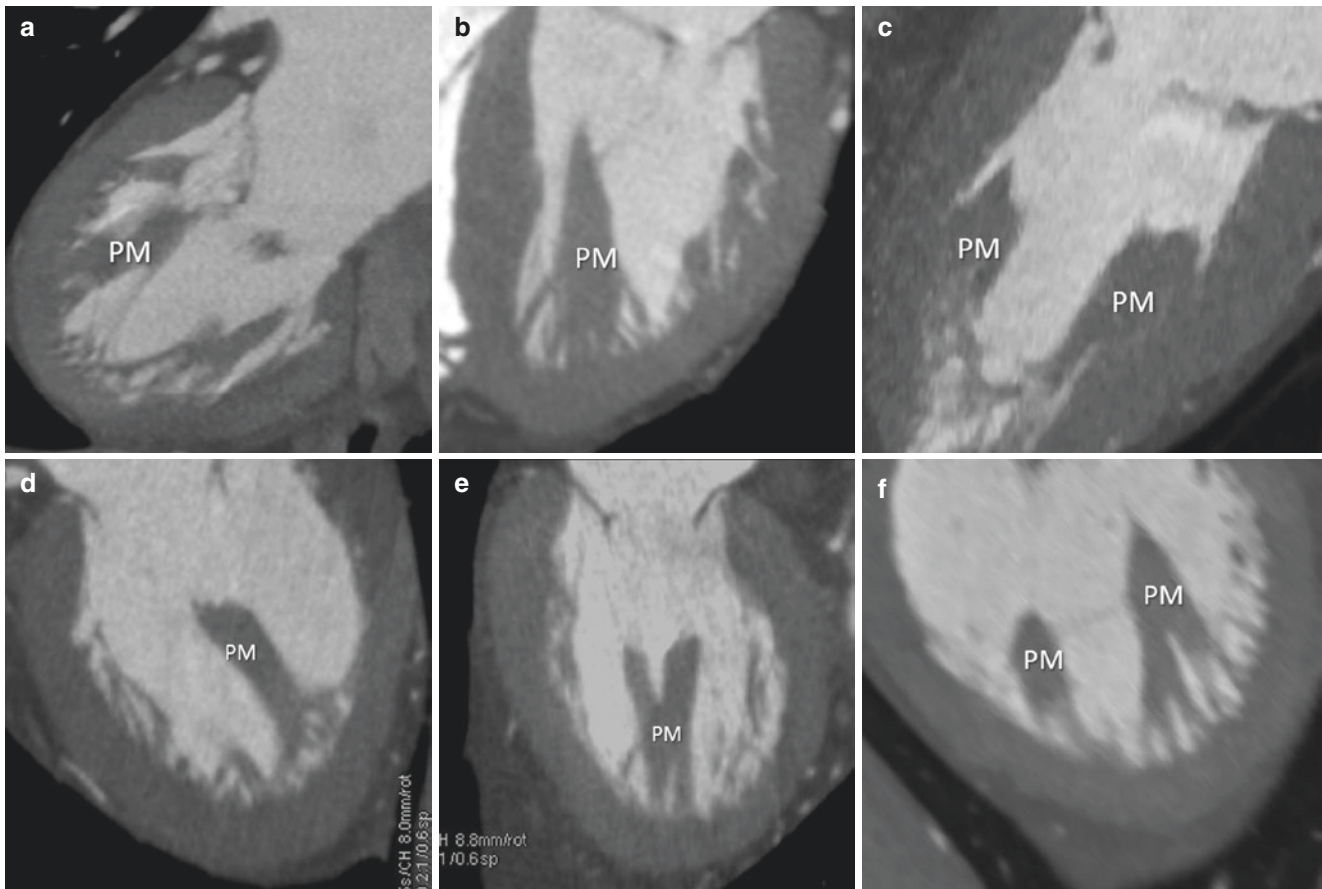


Fig. 6.4 (a–f) CT scan multiplanar images showing different shapes of papillary muscles (PM)

PMs are located near the mitral valve commissures in antero-lateral and posterior-medial position. During systole, contraction of PMs tightens chordae tendineae and prevents prolapse of mitral leaflets. The contraction of PMs is, in fact, essential for maintaining a constant distance between the tip of PMs and the area of coaptation of the mitral valve. When there is any decrease of PM's contraction, chordae tendineae become relatively too long to firmly tightening mitral leaflets at their coaptation line, and as a consequence, leaflets are free to move beyond the annular plane (leaflets prolapse), causing mitral regurgitation. PM dysfunction refers to a condition in which a PM reduces its contractile action as a result of localized ischemia. The immediate consequence is the appearance of mitral regurgitation, which may disappear if the ischemia is transitory.

PMs are usually described as two single pillar-shaped muscular protrusions with one, two, or more heads that are connected with the mitral leaflets through chordae tendineae. In reality, however, the number and shape of PMs can be extremely variable: PMs can be conical, cylindrical, broad-apexed, pyramidal, fan-shaped, flat-topped, truncated, bifurcated, and trifurcated. Finally, muscular bands

may connect the two groups of PMs, although intragroup connections are more frequent. Figure 6.4 shows different aspects of PMs as visualized by the CT.

The connections between PMs and the compact myocardium are particularly important since vessels and nerves reach the PMs through their bases. Moreover, cutting PMs during mitral valve replacement may negatively affect LV function, suggesting that the connection between the base of PMs and the wall is important in determining normal pattern of wall motion. Until few years ago, textbooks and articles depicted the PMs as having a broad base in direct connection with the compact myocardium. In 2004, Axel provided new insights in the anatomy of PMs using the CT scan. In his article, Axel showed CT images that indisputably demonstrate that the base of PMs is attached to the trabeculae rather than directly to the compact myocardium. Acquiring these “innovative” images was made possible by two conditions that are less obvious in pathological or surgical scenarios: (a) the high spatial resolution of CT technique, which has voxels as small as 0.6 mm; and (b) the time of CT images' acquisition at the end of diastole where the spaces between trabeculae that sustain the PM's body are enlarged and

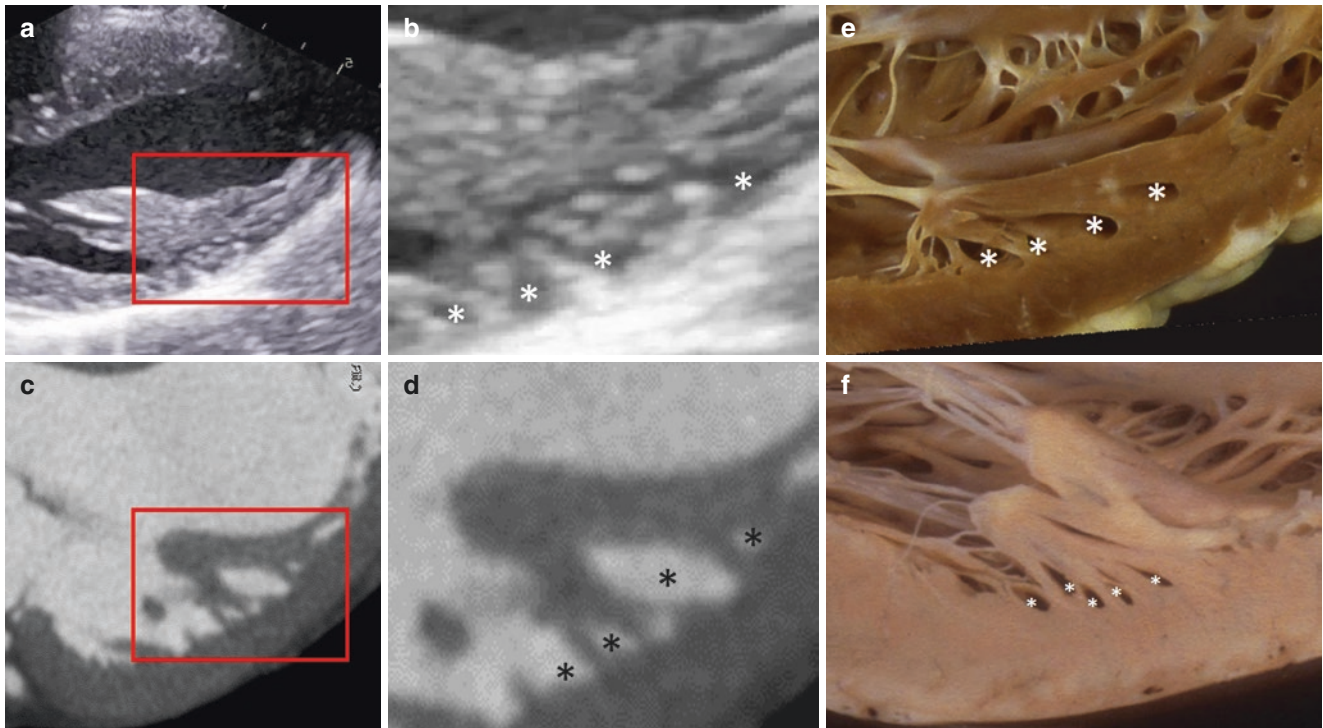


Fig. 6.5 (a) Detail of papillary muscle visualized with 2D echocardiography (a) and CT multiplanar reconstruction (c). The areas in the red box are magnified in (b) and (d) respectively. Images clearly show as the base of papillary muscle attached to the trabeculations rather than

to the compact myocardium. *Asterisks* indicate the inter-trabeculae spaces. (e and f) Anatomic specimens showing the same architecture. *Asterisks* indicate the inter-trabeculae spaces

therefore visible (Fig. 6.5). This is an example of a noninvasive imaging technique that may help in defining fine details of anatomy that were previously disregarded or forgotten.

The arrangement between PMs and myocardium may have functional implications because this mesh-like connection with multiple points of attachment may more effectively reduce the stress on the base of PM than a pillar like attachment. Having a blood supply entering the PM body from several pathways may create a perfusion redundancy that acts as protection against ischemia.

PMs are part of the mitral valve apparatus; thus, readers also will find images and descriptions in Chap. 1.

Microstructure

Understanding LV contraction requires knowledge of the fine microstructure of the myocardium. Description at the “molecular level” of the arrangement of the myocardial fiber is beyond the scope of this chapter. Though prevalently composed by myocytes (nearly 80% of the mass of the myocardium is formed by myocytes), it must be emphasized that the myocardium contains other types of cells (endothelial cells, fibroblasts, and other connective tissue cells, mast cells and immune system-related cells, and pluri-potent “stem cells)

that interact each other and with muscular cells via a variety of paracrine, autocrine, and endocrine factors. Finally, the myocardium is permeated by a diffuse network of connective fibrils (see below), adipose tissues, arteries, veins, nerves, and lymphatics.

Myocytes

The LV myocardium consists of 2–3 billion cells called *myocytes*. The myocyte is a long thin cell of approximately of 100–120 μm in length and 20 μm in diameter and is surrounded by a membrane (sarcolemma). Each myocyte is firmly connected with surrounding cells by *intercalated disks*, either through end-to-end or side-by-side joining. The intercalated discs are part of the sarcolemma and contain two components essential for the myocardial contraction: the *gap junctions* and *desmosomes*. The gap junctions are channels between myocytes that directly link the cytoplasm of adjoining cells and provide a relatively unrestricted passage of ions. The gap junctions between myocytes form a complex three-dimensional network of anastomosing cells, a sort of *syncytium*. The *desmosomes* are a complex arrangement of proteins across two adjacent sarcolemma that anchor them together so they do not pull apart during the contraction of individual myocytes. Myocytes characteristically contain an

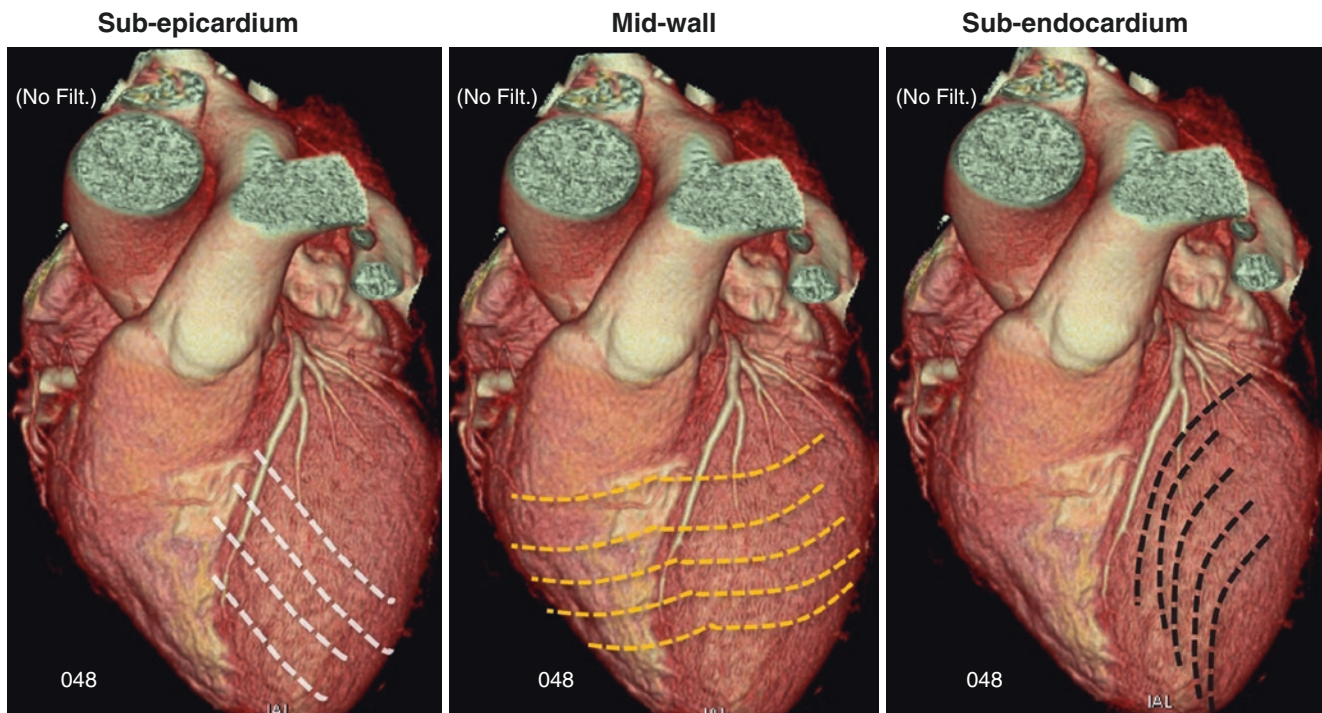


Fig. 6.6 CT scan volume rendering format with superimposed line of prevalent orientation of myofibers in sub-epicardium, mid-wall, and sub-endocardium

impressive number of mitochondria that produce high levels of ATP. In any myocyte the sarcolemma projects long, finger-like invaginations called *T-tubules* into the cytoplasm. The T-tubules join sacs or channels of *sarcoplasmic reticulum* in a way that two sacs of the reticulum are positioned laterally to a single T-tubule (the so called *triade*). This configuration is the anatomical basis of excitation-contraction: indeed, when a positively charged current is transmitted from the *neuromuscular junction* it runs down to the T-tubule. The influx of calcium activates receptors of the adjacent sacs, which initiate a release of calcium ions. Calcium ions, in turn, activate a precise cascade of events consisting of complex rearrangements of several molecules, which eventually leads to a contraction (see below).

The *myofibrils* are undoubtedly the fundamental structure of myocyte. About 80% of the sarcoplasm of myocytes is occupied by myofibrils. Myofibrils are substantially linear structures that resemble cables running parallel to the long axis of the myocytes. They are made up of millions of *sarcomeres*, the true “engines” of the contraction. The sarcomere is about 3 μm in length and each myofibril contains thousands of sarcomeres that together cover the entire length of the myofibril. The sarcomeres are connected end-to-end at the so-called *Z-line*. Each sarcomere contains thick and thin myofilaments called *myosin* and *actin* respectively, interdigitated with one another. The Z-line acts as scaffold connecting thin filaments from adjacent sarcomeres. Myosin and actin are interconnected with a series of specialized proteins

(myosin, myosin binding protein-C, titin, actin, troponin, tropomyosin, nebulin, and others) which contributes to the shortening and lengthening of the sarcomere. The capability of sarcomeres for shortening and elongating rhythmically occurs when these parallel thick and thin filaments slide with each other thanks to “cross bridges” that form in presence of ATP. In other words, the filaments of actin protein form the “ladder” along which the filaments of myosin “climb” to generate motion. These small “engines” have the capability of shortening up to 30–35%. Under physiological conditions, however, a shortening of only 10–20% is necessary (Figs. 6.6 and 6.7).

The Extracellular Matrix

The *extracellular matrix* is another fundamental component of the myocardial structure. A fine network of collagen fibers called *endomysium* wraps each myocyte, reinforces the role of intercalated discs in binding myocytes to one another, thus preventing the slippage between cells, and acts in such a way that it synchronizes the transmission force between myocytes. The *perimysium* is a more robust and thicker network of connective fibers that groups thousands of myocytes into the so-called *myofibers*. Moreover, lateral connective strands anchor myofibers to each other, preventing a malalignment. Blood and lymphatic vessels, and fibers of the conduction system that serve the myocytes, run in the perimysial space

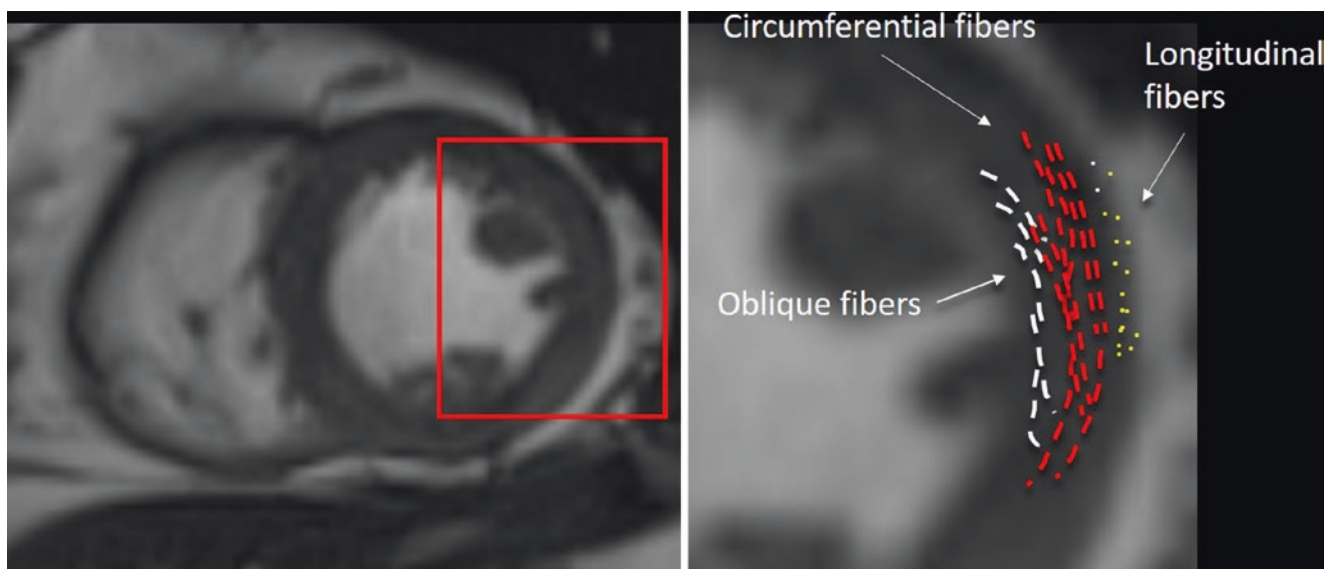


Fig. 6.7 CMR image in short-axis view. The area in the red box is magnified to the right. Directional lines of myofibers are depicted in white in the sub-endocardium, in red in the mid-wall, and in yellow in the sub-epicardium

between myofibers. A perimysial sheet allows the myofibers to slide alongside one another during the cardiac cycle (see below). Finally, myofibers are packed together by the *epimysium*, which surrounds the entire myocardial mass.

Relation Between Myocardial Structure and Function

The relationship between myocardial structure and myocardial function has been debated for several decades, if not centuries. Several hypotheses have been described, ranging from laminar sheets, layered fibers, complex nested syncytium, to a unique band arrangement organized in two distinct helicoids. Nowadays, most anatomists and physiologists agree that the ventricular mass is arranged on the basis on an interweaving network of myofibers. Moreover, two helical fibers arrangements have been recognized: a right-handed helical arrangement that takes place in the subendocardial region with an angulation respect to the longitudinal axes of $+60^\circ$, and a left-handed helical configuration in subepicardial regions (-60°). Thus, the majority of subepicardial myocardial fibers overlap those of subepicardium with an angle of 120° . In the subepicardium, myocardial and in papillary muscles fibers may also run vertically. This counter-directional arrangement of myocardial fibers maintains stability and minimizes energy expenditure. At mid-wall, halfway between epicardium and endocardium, myocardial fibers lie in the circumferential plane aligned with short axis sections and perpendicular to long axis planes. It must be said that these three layers are not at all separated by cleavage planes since myofibers of one layer are interconnected

with myofibers of an adjacent layer. Thus, the overall histological picture is that of a meshwork.

Recent advances in cardiac magnetic resonance allow direct visualization of the myocardial fiber architecture using diffusion tensor imaging. This novel method has emerged as the gold standard for “nondestructive” reconstruction of fibers orientation (in opposite to “destructive” studies when dissections of anatomic specimens are used). This is based on the principle that the main orientation of the fibers parallels the diffusion of water molecules, which causes a signal attenuation in the presence of a magnetic field. This method allows the capture of impressive images of the actual arrangement of fibers *in vivo*.

Thickening, Longitudinal Shortening, and Torsion

The LV is capable of ejecting during exercise more than 100 mL of blood (which is viscous liquid) against over 200 mmHg, and then receiving the same quantity at less 10 mmHg and in less than 100 ms. This incredible performance is possible because during systole the LV myocardium thickens radially, shortens along meridians, and the apex twists relative to the base.

Ventricular *wall thickening* is an important mechanism for systolic ejection, accounting for 25–50% of stroke volume. Myocardial fibers, myocytes, myofibrils, and sarcomeres have an “elongated” appearance. It is therefore intuitive to suppose that they are structured to shorten along their major axis. In a cascade of events, shortening of the sarcomere should cause shortening of the fibril and, subsequently, a

shortening of the myocytes and myocardial fibers. However, since myocardial fibers are arranged almost parallel to the endo, meso, and epicardial surfaces of the LV, the wall thickening must take place not only because fibers shorten but also because they “thicken.”

During systole the ejection fraction of LV is 50–70%, and the increase in wall thickness is 30–50%. Both vastly exceed sarcomere thickening that is only 10%. How can the wall thickness increase by 30%, while the fibers thicken only 10%? Indeed, increase in cell diameter (thickening) as myocytes shorten, would contribute only about one fifth of the thickening of the wall. Moreover, while the shortening of the fibers is substantially the same from the epicardium to the endocardium and from the apex to the base, the parietal thickening is greater in the inner than in the outer layers.

There is an almost universal agreement among anatomists that the ventricular myocardium has a laminar organization in which myocytes are grouped into branching layers (three to six cells thick) surrounded by an extensive perimysial collagen network and separated by sheet cleavage planes.

Though significant regional variations in the organization of the laminae may exist, this structure provides a rational explanation between arrangement of myocytes and systolic wall thickening. Indeed, it can be observed that these myocardial *laminae* assume in diastole an oblique direction from top to bottom and from the outside toward the inside. In systole, the laminae slide one on the other along the cleavage planes, assuming a direction more perpendicular to the long axis of the ventricle. This change of direction is probably determined by the contraction of the longitudinal fibers present in the subepicardium and subendocardium. Thus, the thickening of the wall does not take place only because millions of fibers shorten and thicken, but also because of a rearrangement of myocardial laminae: in systole the laminae are arranged more “perpendicular” with respect to the long axis of the ventricle, and in this way they increase the wall thickness. The laminar myocardial structure with sheets of myocytes separated by cleavage planes seem to be appositely designed for a radial thickening. Obviously, the opposite occurs in diastole (Fig. 6.8).

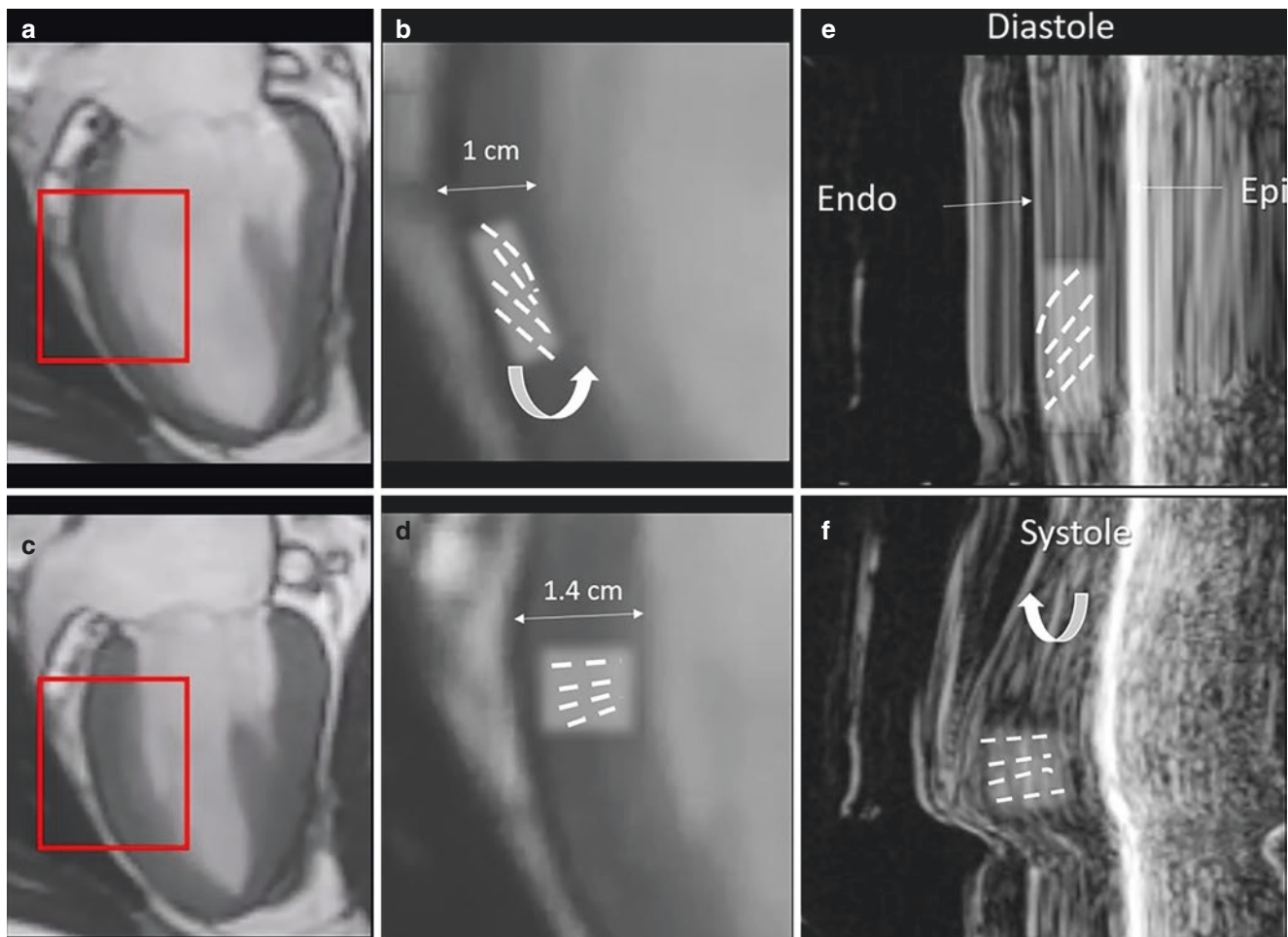


Fig. 6.8 CMR images in long-axis view in diastole (a) and systole (c). The areas in the red boxes are magnified in (b) and (d) respectively. The superimposed dotted lines show the “laminae” that in diastole assume an oblique direction from top to bottom and from the outside toward the inside. In systole the laminae slide one on the other along the cleavage

planes, assuming a direction more perpendicular to the long axis of the ventricle. *Curved arrow* marks the direction of the motion. (e–f) M-Mode echocardiography showing the radial thickening of the posterior wall in one point. *Dotted lines* represent the disposition of laminae in diastole (upper half of the figure) and in systole (see text)

Longitudinal shortening occurs because of contraction of sub-endocardial and sub-epicardial oblique/longitudinal fibers. Because the apex is firmly attached to the diaphragm, the longitudinal shortening leads to the descent of the atrioventricular and aortic valve planes (Fig. 6.9). It is interesting to note that the aortic and mitral translation toward and away from the LV apex determines a passive displacement of a column of blood across the valves. The diastolic translation of mitral annulus away from the apex, for example, promotes LV filling by displacing the column of blood initially present in left atrium to underneath the mitral leaflets. In systole, the translation of mitral plane toward the apex enlarges the left atrium with a consequent drop in atrial pressure. This atrial “vacuum” promotes the pulmonary venous return. In the absence of longitudinal shortening, as occurs in hypertrophic or infiltrative cardiomyopathies, the left atrium does not enlarge, and the left atrial pressure remains high, preventing a regular inflow of blood from the pulmonary veins with increase of pulmonary capillary pressure and consequent transudation into the interstitial space. This mechanism causes symptoms of heart failure. Of note, this may occur in the presence of preserved ejection fraction since the systolic contraction may be maintained by the radial thickening, the so-called “heart failure with preserved ejection fraction.” On the other hand, the motion of the aortic root toward the apex displaces the column of blood from the outflow tract to the aorta, increasing the systolic stroke volume.

Twist, untwist, rotation, torsion—these terms have been used in the literature to describe systolic rotation and diastolic reverse rotation of the LV base and apex as viewed from the apex. In other words, the LV has a “wringing” motion (Fig. 6.9).

The contraction of subendocardial myofibers should rotate the apex in opposite directions. The outer subepicardial layers dominate the overall direction of rotation; however, myocardial activation occurs first in the subendocardial layers, which therefore shorten earlier, stretching the subepicardial layers during the isovolumetric phase, causing a brief LV un-twist. During the ejection period, the subepicardial layers dominate the direction of the rotation. Of note is the role of the myocardial connective network: during systole, myocardial contraction stretches the connective fibrils. The stored energy is released during diastole, facilitating a diastolic recoil. LV mechanics can be assessed non-invasively using echocardiography (in particular, speckle tracking) and cardiac magnetic resonance using tissue tagging.

The Role of Blood

LV is considered as a pressure generator. Thinking of the LV as a “hydraulic pump” derives from the concept that the blood is an inert, amorphous liquid that must be pushed “by force” into the circulation. The concept of the heart as a generator of pressure in the cardiological community has been imposed by the fact that most of our knowledge in terms of

the physiology of the cardiovascular system is essentially derived from the measurement of hemodynamic pressure curves. As mentioned, the singular arrangement of myocytes in laminae and helical configuration allows a complex contraction where radial thickening, longitudinal shortening, and apical twisting act together for generating a systolic pressure to push the blood through arterial vessels. However, there is still ongoing debate on the “energetic sustainability” of the myocardium in doing this work. Indeed, 300 g of muscular tissue must be able to “push” thousands of liters of inert blood every day (with a viscosity five times greater than that of water) through billions of arterioles and capillaries (whose last dimensions are not greater than the diameter of the erythrocytes). Moreover, the anatomy of the ventricular cavity would appear to be not completely suitable for being a “generator” of pressure. The apex, for example, has a considerably thinner wall than the base and is therefore more subject to the action of intraventricular pressure (Fig. 6.10).

The hypothesis of an additional source of energy generated directly by the blood itself (which then is no longer an inert liquid) is fascinating. In the fetal period when the heart is still a tube and does not generate pressure, the blood advances like a liquid cylinder rotating with a spiral movement along the axis of advancement. The propulsion force is given by the movement of the blood itself, which advances by virtue of its rotary movement (like a vortex). In the early stages of development, the blood rotating in the cardiac cavity would transfer its momentum (i.e., mass \times speed) to the muscle. In this way, the blood momentum would combine with that of the heart, favoring rotation and propulsion. In other words, the spiraling structure and movement of the heart would be the consequence of the inherent spiraling movement of the blood, and not vice versa. This is a general tendency of liquids that, in nature, tend to move in a spiral way (just see how the water goes down the sink to reach the drain). The heart with its contraction would favor and perpetuate this rotational movement by minimizing energy expenditure. It is possible that the structure of the cardiovascular system has specialized in the course of millions of years to obtain the maximum benefit from this propensity of liquids (including blood) to flow in a spiral-like manner.

A sort of “electronic cast” can be obtained with CT making transparent the myocardium and increasing the opacity of intracavitary contrast. These electronic casts characteristically show a helical disposition of trabeculations. Whether arrangement is “sculptured” by the spiral movement of the blood is unknown (Fig. 6.11).

The Right Ventricle

In 1943 Star et al. noted that major destruction of the right ventricle causes only minimal changes in venous and arterial pressure. Similar studies later confirmed that extensive dam-

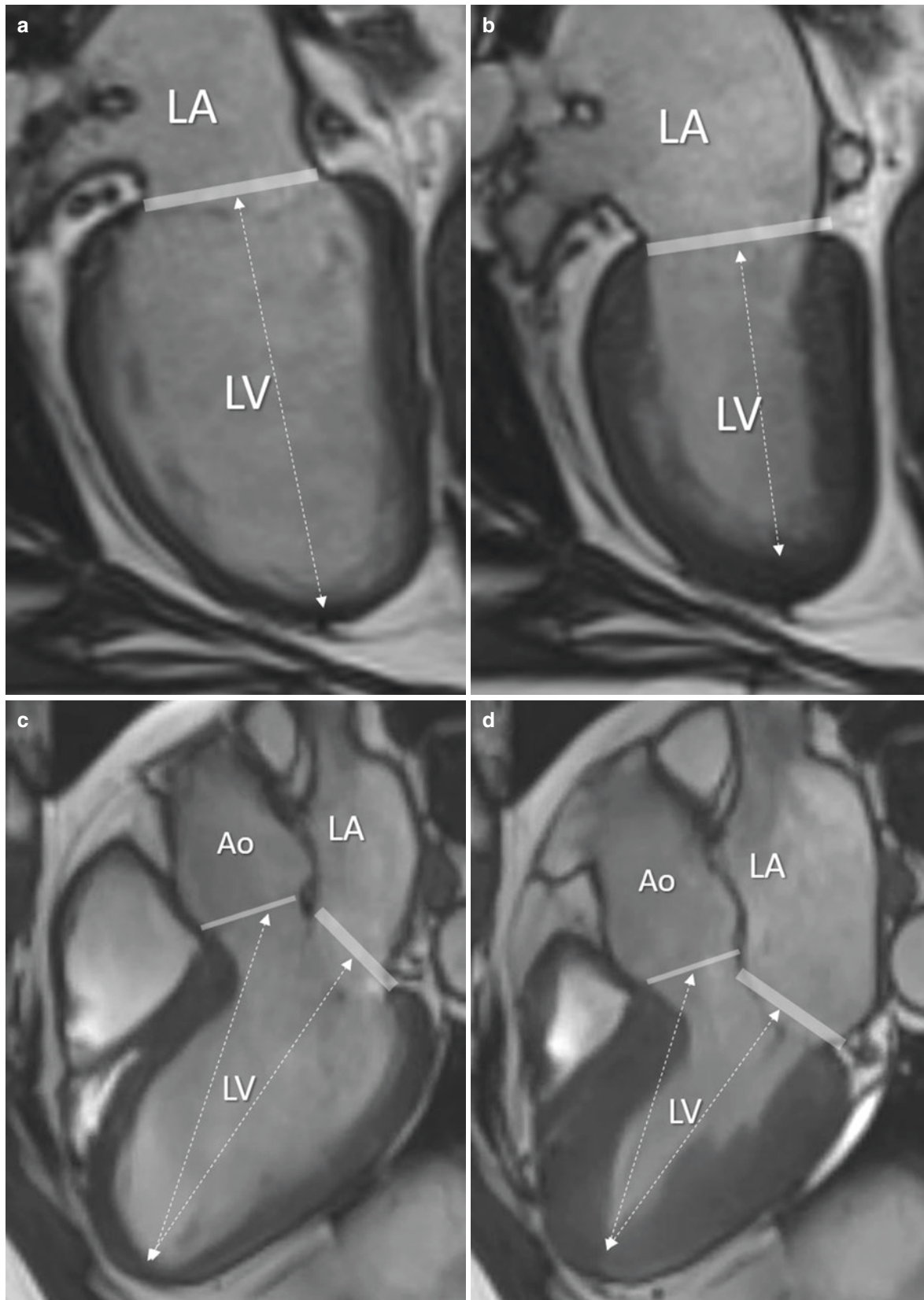


Fig. 6.9 Longitudinal shortening assessed by CMR in two chamber view (a, b) and long-axis view (c, d). Because the apex is stationary, the longitudinal shortening produces the atrio-ventricular (*thick line*) and

aortic (*thin line*) planes to descend toward the apex. *Dotted double arrowlines* mark the distance between mitral and aortic planes and the apex in diastole (a, c) and in systole (b, d)

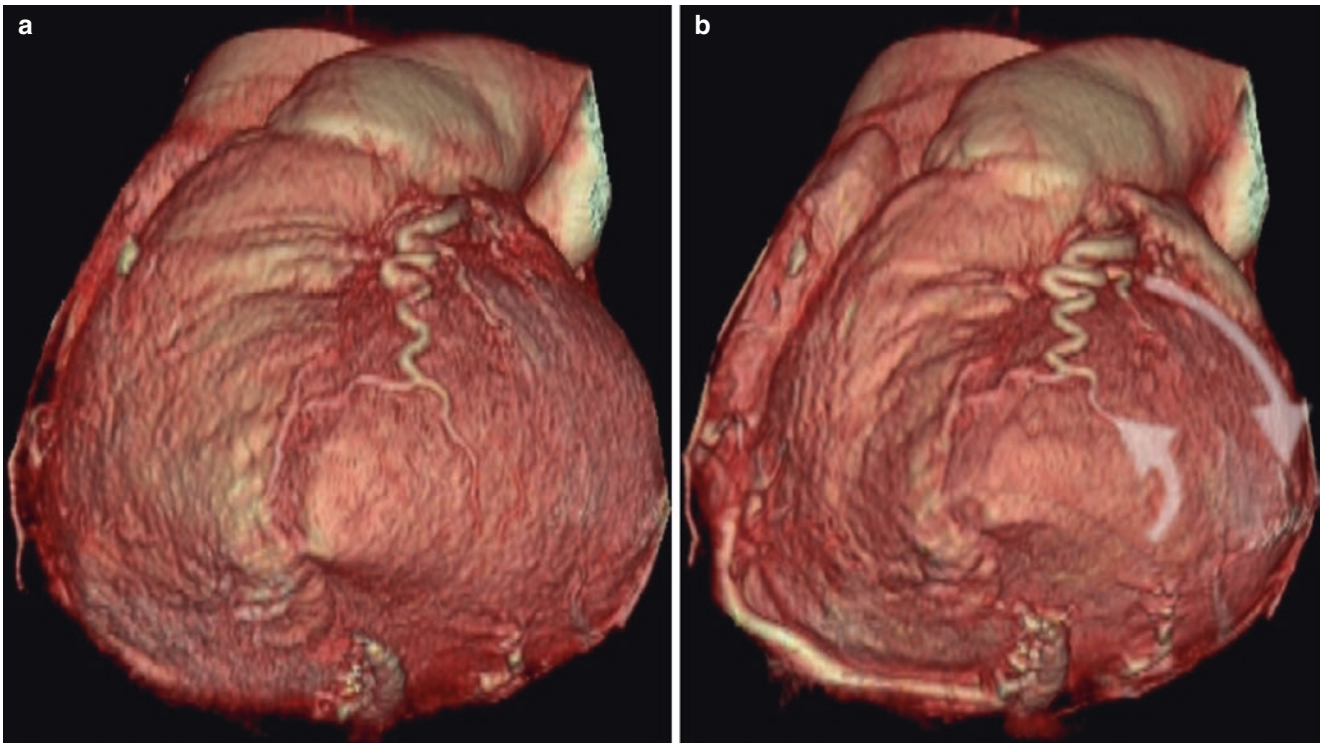


Fig. 6.10 CT scan volume-rendering format of the ventricles seen from the apex in diastole (a) and in systole (b). *Curved arrow* indicates the counterclockwise rotation of the apex and the clockwise rotation of the base

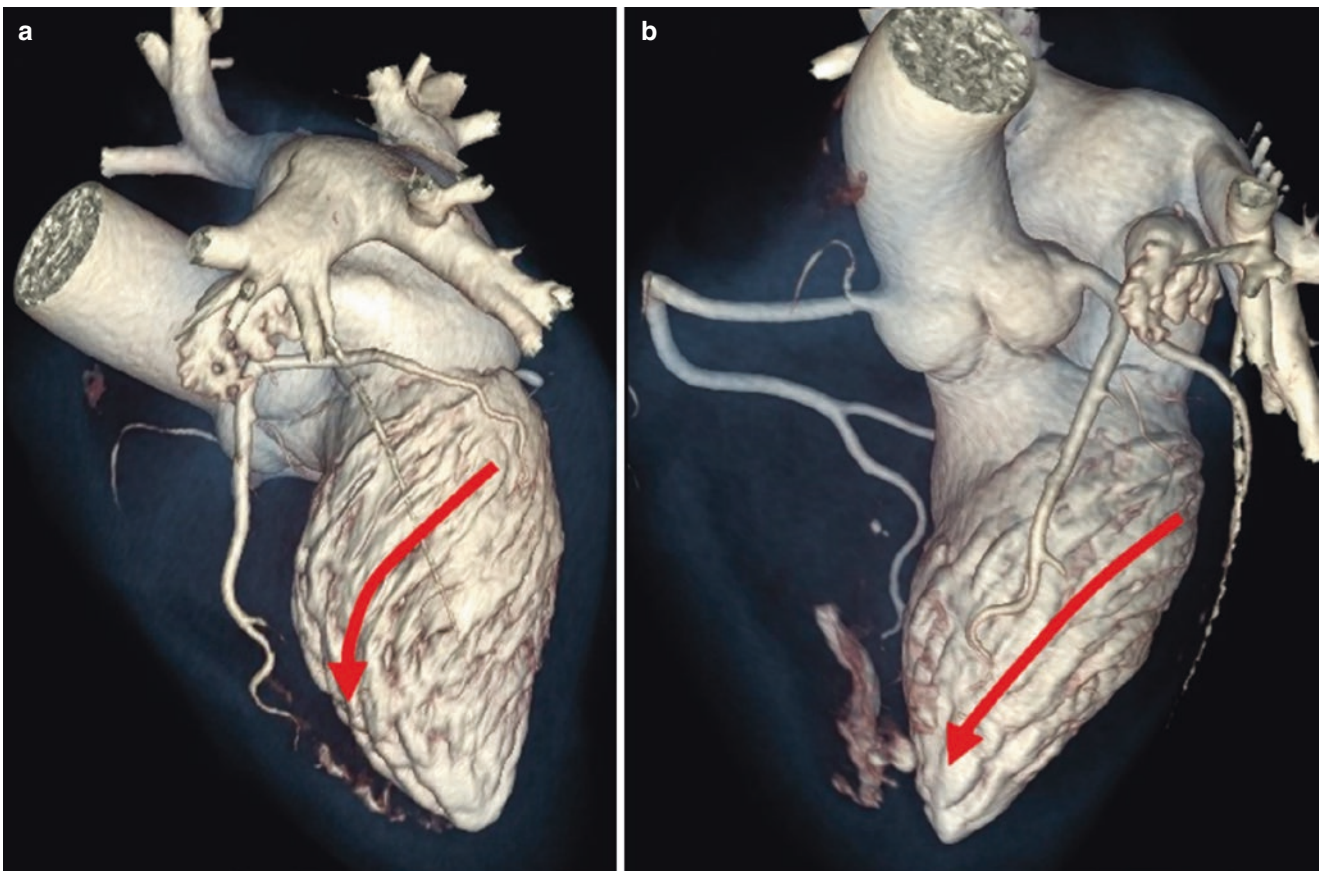


Fig. 6.11 (a and b) Electronic cast obtained by CT scan making transparent the myocardium and opaque the contrast into the LV cavity. These casts show a helical arrangement of trabeculations (*curved red arrows*)

age of RV does not produce right heart failure and venous congestion. Thus, in the middle of the nineteenth century, the leading opinion was that a normal contractile RV wall is not necessary for the maintenance of a “normal circulation.” Today we know that, in case of a failure of RV, contraction of the LV may indeed support the circulation, though for a limited period of time, with the contraction of interventricular septum (see below). The belief that the RV had substantially negligible clinical relevance was further reinforced by the use of Fontan surgical procedure in patients with tricuspid atresia and rudimentary RV or other so-called univentricular hearts. The surgical intervention consists of diverting the venous blood from inferior and superior vena cava to the pulmonary arteries by creating a total cavo-to-pulmonary arterial communication that completely excludes the RV from the circulation.

Like the tricuspid valve, the RV therefore became a “forgotten” chamber and was disregarded by the cardiology community for decades. Only a couple of decades ago accumulating evidence emphasized the relevance of RV in almost any cardiac scenarios, for both its clinical impact and its prognostic implications. Herein we present an update of the normal RV anatomy, as we believe that a detailed knowledge of RV anatomy is an indispensable prerequisite to understand RV abnormalities, and is also valuable for electrophysiologists during their invasive procedures and device implantations. Finally, we conclude the chapter by describing the anatomy of the pulmonary valve.

Location and Shape of the RV

Situated directly behind the sternum and anterior to LV, the RV is a thin-walled crescent-shaped ventricular chamber (Fig. 6.12).

From an anterior-posterior perspective the RV appears to have a triangular/trapezoidal shaped aspect. Along its transverse axis the RV curves antero-superiorly, wrapping around the LV (Fig. 6.13). This complex anatomy cannot be fitted to simple geometric models, and this is the major limitation for understanding RV volume and function when it is measured in two-dimensional tomographic views.

This shape, as well as the fact that the two ventricles share the interventricular septum, pericardium, and myofibers (especially their superficial layers) explain the phenomenon of the “interdependence” of the ventricles. Indeed, while the RV has little or no effect on the LV contraction, roughly 30% of the contractile energy of the RV is generated by the LV which, through the septal contraction, contributes significantly to RV pressure generation.

In the normal adult heart, the wall of the RV is considerably thinner than that of the left ventricle, ranging from 3 to 7 mm, but being as thin as 1.5 mm at the tip of the apex. The RV appears therefore quite vulnerable to perforation by catheters and pacemaker leads positioned near the apex (Fig. 6.14b). Accordingly, the RV mass is about one-sixtieth that of LV mass. Nevertheless, in normal conditions, the RV is perfectly adequate for ejecting blood in a low impedance pulmonary vasculature. Owing to its thinner wall, the RV has a greater compliance than the LV. Because of these anatomical characteristics, it is perfectly comprehensible that the RV tolerates volume overload better than pressure overload (Fig. 6.14).

Inlet, Apical Trabeculated, and Outlet

In the normally developed RV, with normal atrioventricular and ventriculoarterial concordance and normal tricuspid and pulmonary valves, the RV can be divided into three major regions: inlet, apical, and outlet, although no clear anatomical demarcations can be seen between these parts (Fig. 6.15a). The inflow/outflow axis angle of the RV is significantly wider than that of LV. This anatomical architecture requires that the right outflow tract must contribute to the overall RV ejection fraction (see below) (Fig. 6.15b). Interestingly, the RV outflow tract has a different embryological origin than the remaining RV myocardium.

The *inlet component* surrounds and supports the tricuspid valve and its subvalvular apparatus extending from the hinge line of tricuspid valve up to the insertion of papillary muscles (Fig. 6.15a). The *apical component* is characterized by trabeculations that are thicker than the counterpart LV trabeculations. These coarse trabeculations may help to distinguish the “morphological” RV from the morphological LV irrespective of the position of the chamber within the heart.

The *outlet component* or infundibulum consists of a muscular “freestanding” tube-like portion, free of trabeculations, which supports the pulmonary valve. It accounts for nearly 20% of the right volume. The posterior aspect of the RV outlet is formed by the supraventricular crest (see below). Interestingly, the RV outlet is separated from the aorta by a cleavage plane filled with epicardial fat. Thus, the RV outlet can be removed surgically without entering in the LV cavity (Fig. 6.16).

This particular anatomical configuration allows retrieval of the patient’s own pulmonary valve with its muscle sleeve to replace the patient’s diseased aortic valve in the Ross procedure. The pulmonary valve is then replaced with a pulmonary allograft. This is the procedure of choice in children and infants with aortic valve disease.

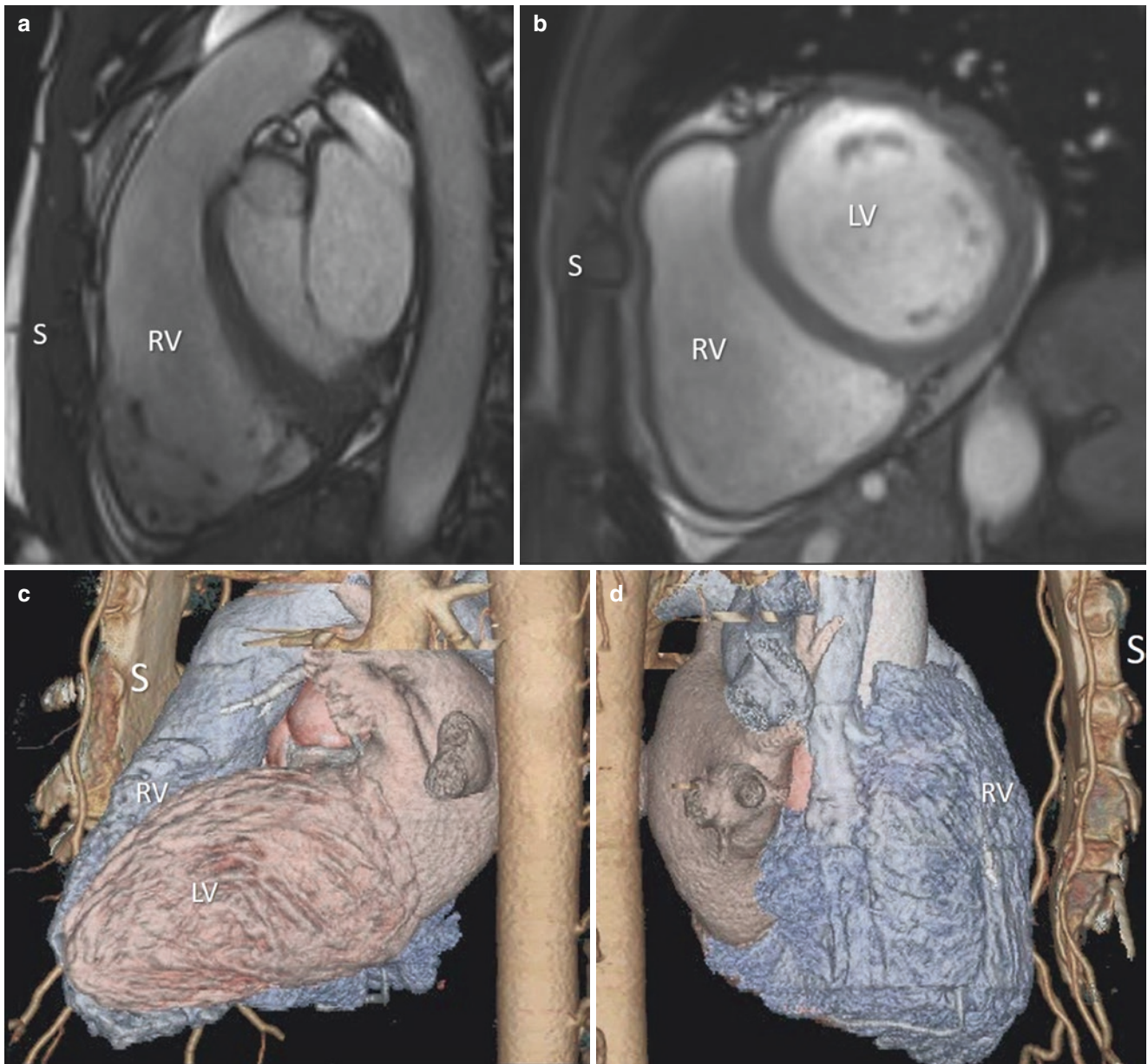


Fig. 6.12 CMR in longitudinal (a) and cross-sectional (b) view and CT electronic casts (c and d) in two different perspectives showing the right ventricle (RV) anterior to left ventricle (LV) located just behind the sternum (S)

Specific Anatomic Structures

Within the RV cavity three structures are peculiar to the RV: the supraventricular crest, the septomarginal trabeculation, and the moderator band.

The *supraventricular crest* is a prominent muscular structure that forms the posterior wall of the RV outlet and separates the inlet from the outlet components of RV. Indeed, contrary to the left side where the aortic and mitral valves are adjacent to each other and connected by a fibrous band (see Chap. 1), the

tricuspid and pulmonary valves are widely separated by this muscular wall. In cross-section at its septal origin, the supraventricular crest looks like a semilunar ridge with the origin of the right coronary artery on its epicardial aspect. Seen from an external perspective it is clear that it is an infolding of the RV wall (the ventricular-infundibular fold) that extends from its septal origin, accommodating the aortic root, and tapers as it extends parietally. As mentioned, a space (often virtual) filled by a leaf of epicardial fat separates the supraventricular crest (and the infundibulum) from the aorta (Fig. 6.17).

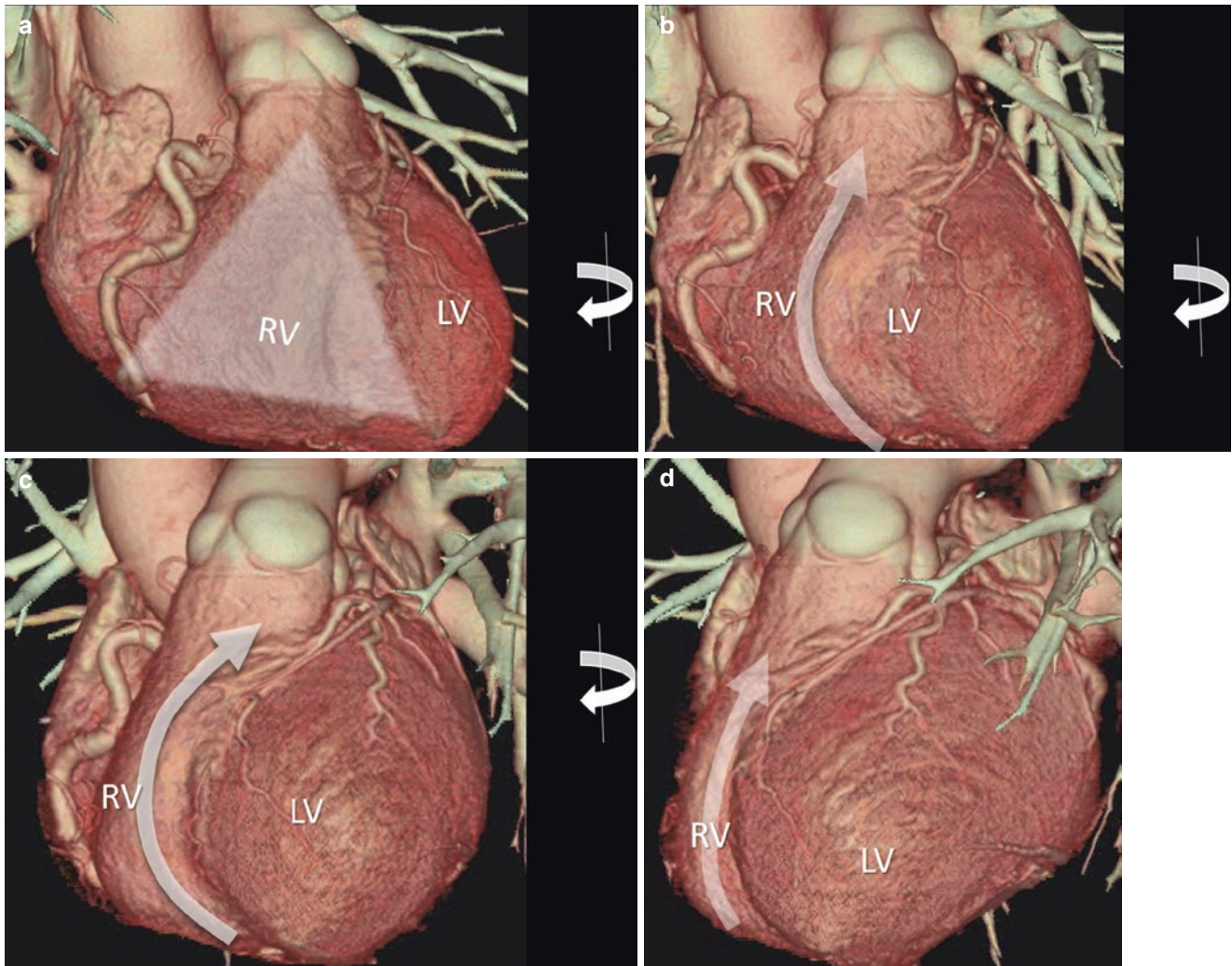


Fig. 6.13 (a–d) CT scan volume rendering showing as in antero-posterior perspective (a) the RV has a triangle-shaped aspect. By rotating the image from right to left around the y-axis (curved arrow), it appears that the RV wraps around the LV (curved arrows)

The term *septomarginal trabecula* (SMT) was first use in 1913 by Tandler, who noted that this muscular band was attached proximally to the septum and distally to the margin of RV. Indeed, the SMT is a muscular column protruding from the septal surface beginning below the supraventricular crest and continues toward the anterolateral wall of the RV joining, through the moderator band (see below), the base of anterior papillary muscle (see also Chap. 3 on the tricuspid valve).

While superiorly the SMT bifurcates in two arms that embrace the ventriculo-infundibular fold forming the supraventricular crest, the column-like body extends toward the ventricular apex, where it gives origin to the *moderator band* (MB).

The MB takes its name as a result of a supposition that it may control or “moderate” an excessive dilation of the RV when too much blood fills it. Indeed, it has a characteristic course crossing the right ventricular cavity and ends at the base of anterior papillary muscle, where it attaches to the RV free wall.

Interestingly, the right bundle branch of the conducting system runs through the subendocardium of the SMT and the MB carries a significant sub-branch across the RV cavity to the parietal RV wall. The SMT, the moderator band, and the anterior papillary muscle form a “U-shaped” protrusion into the RV cavity that separates the inflow from the outflow. Abnormal hypertrophy of these structures may potentially lead to an intracavitary obstruction dividing the RV into two chambers, one proximal at high pressure and one distal at low pressure (double-chambered RV) (Fig. 6.18).

Microstructure

Normal myocytes of RV appear smaller than the LV myocytes, while the RV contains more extracellular matrix in terms of collagen fibers. Characteristically, while the LV myocardium has three distinct layers, anatomical dissections of the RV reveal only two layers: the subepicardial

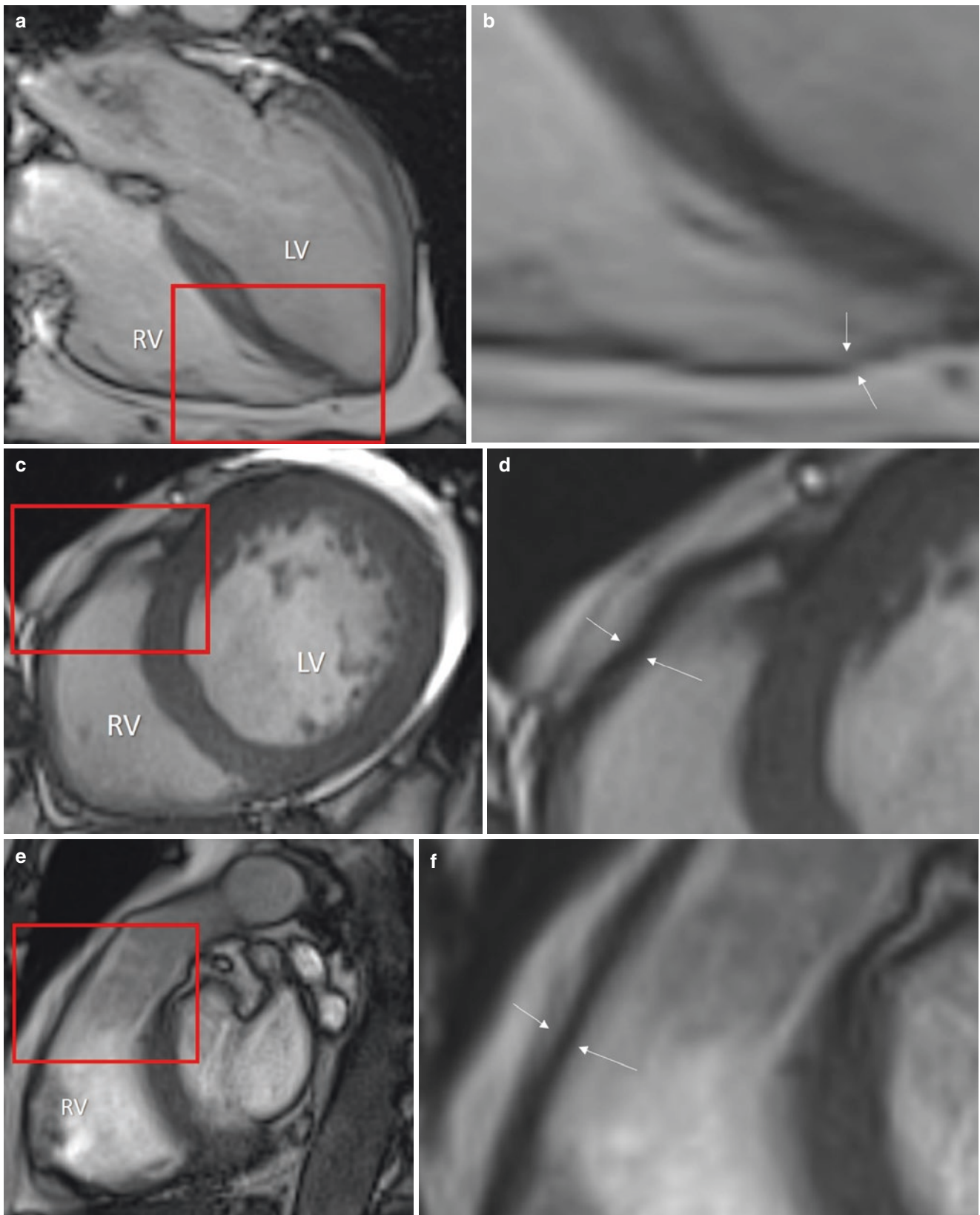


Fig. 6.14 CMR four-chamber (a), short axis (c), and outflow tract (e) sections of the right ventricle (RV). The areas in red boxes are magnified in (b), (d), and (f), respectively. The images show the RV wall (arrows) is significantly thinner than the left ventricle (LV) wall, especially at the apex (b)

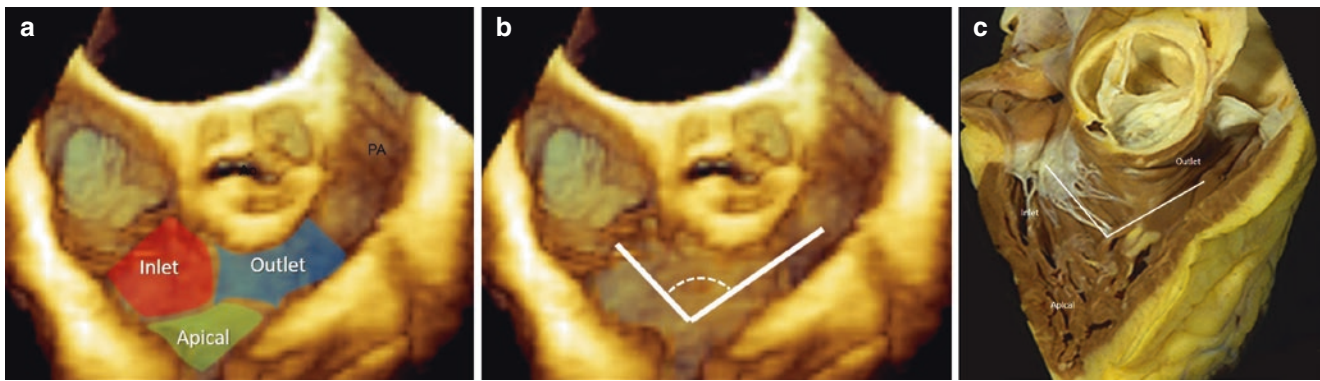


Fig. 6.15 3D TEE (a) showing the three regions of the right ventricle (inlet, apical, and outlet marked with red, yellow, and blue respectively) and the angle between inlet and outlet (b). (c) The corresponding anatomical specimen

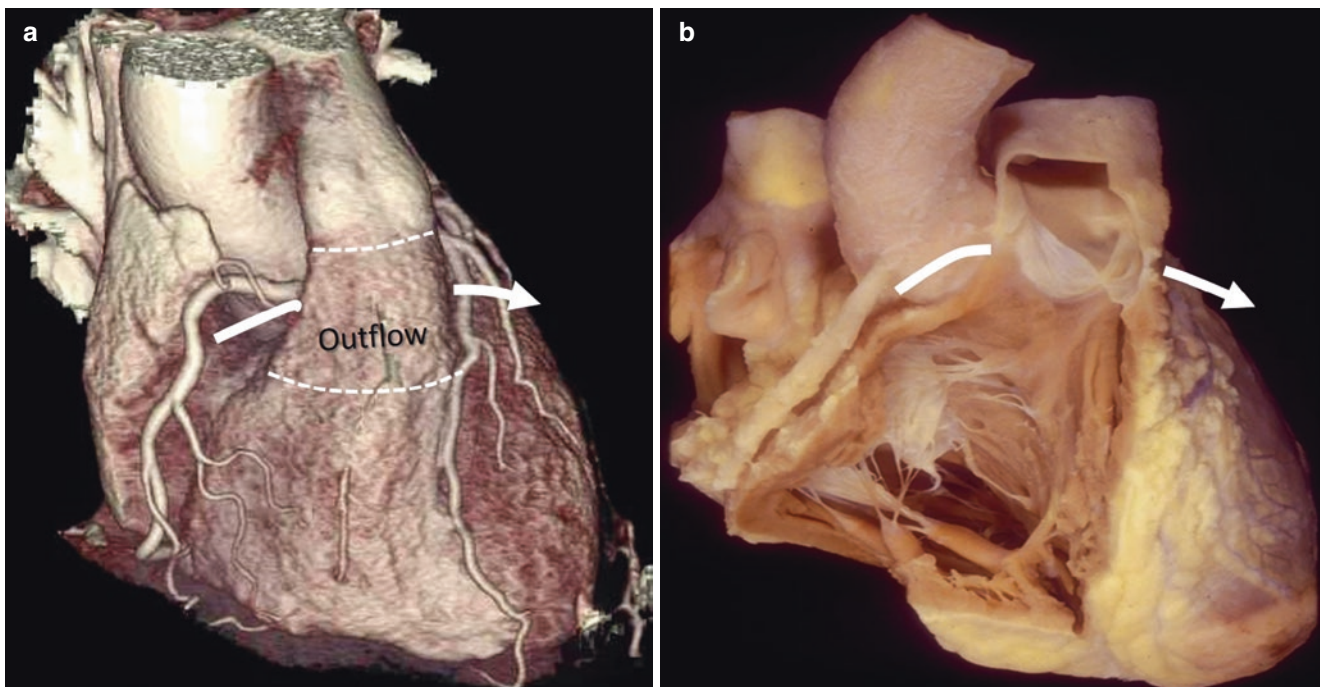


Fig. 6.16 (a) CT volume rendering showing as a cleavage plane (*curved arrow*), separates the RV outflow tract from the aorta and left ventricle. (b) The corresponding anatomical specimen

layer formed by oblique fibers almost parallel to the atrio-ventricular groove, and the subendocardial layer where fibers are preferentially arranged in an oblique fashion (Fig. 6.18).

The Subvalvular Apparatus

Although classically the PMs of the right ventricle have been described as comprising three blocks (septal, anterior, and inferior [or posterior]), this is not always the case. Indeed, the RV PMs are highly variable in number, position, and size. The anterior PM is quite large, frequently unique or

bifid. It is consistently found in anatomic specimens. The inferior PM usually consists of two or three thin PMs originating from the inferior and posterior RV wall. Characteristically, several chordae tendineae attach to the septal leaflet and originate directly from the septal wall. But at the commissure between septal and anterior leaflets, the fan-shaped commissural cord is attached to a septal PM, which is better known as the medial/conal PM or muscle of Lancisi. Originating from the posterior limb of the SMT, it is small and sometimes inconspicuous (see Chap. 3 on the tricuspid valve). As for the left PMs, the right PMs do not attach directly to the compact myocardium but originate from the trabeculations.

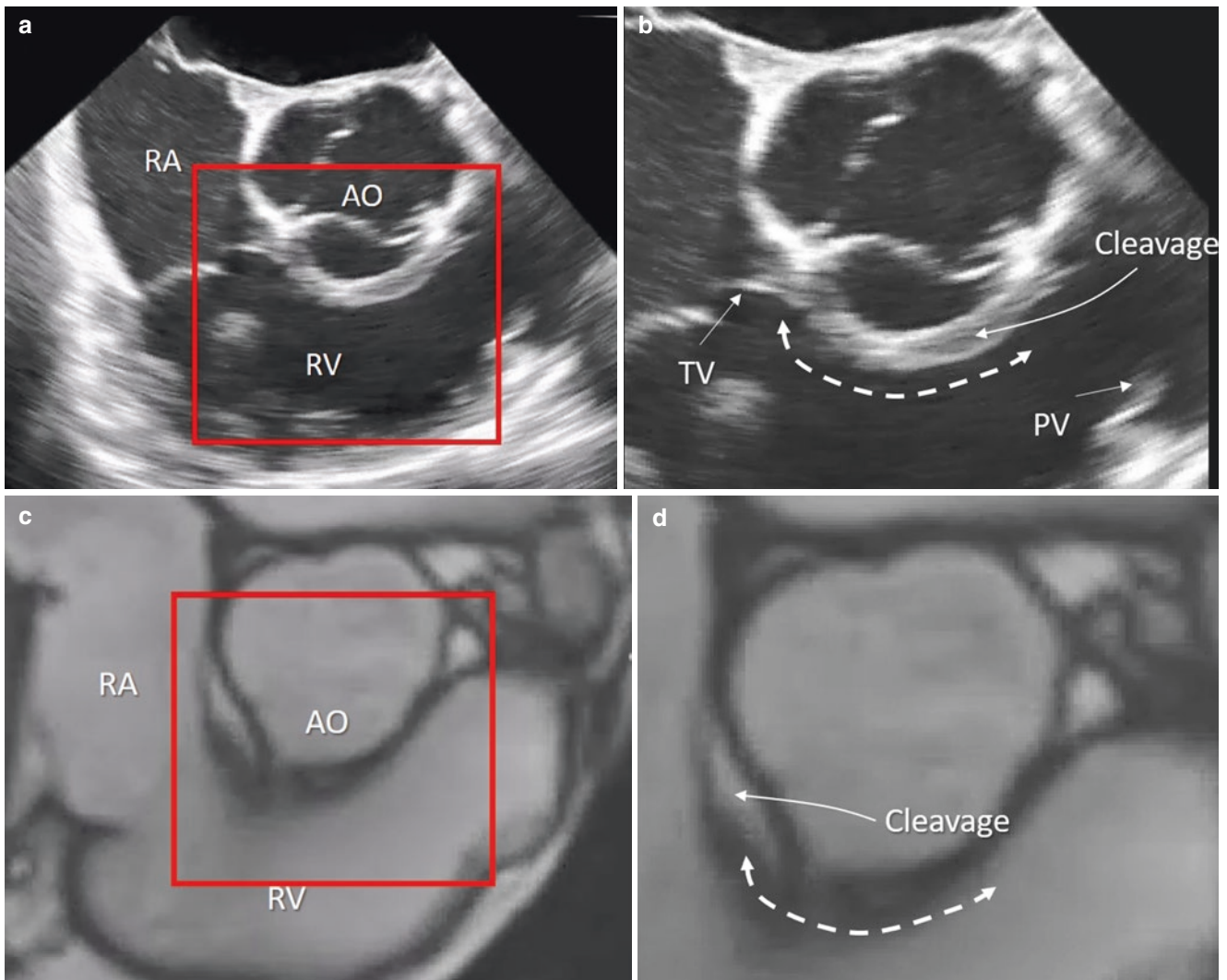


Fig. 6.17 Images obtained with 2D TEE (a) and cardiac magnetic resonance (c). The areas in red boxes are magnified in (b) and (d) respectively. The double arrows mark the extension of the supraventricular crest from the tricuspid to the pulmonary valve. Images clearly

show that the supraventricular crest is an infolding of the RV wall that accommodates the aortic root. The supraventricular crest is separated from the aortic root by a cleavage plane filled by epicardial fat

Pattern of RV Contraction

Knowledge of RV function is still incomplete and certainly behind what we know about the LV. Herein, we present knowledge on the pattern of RV contraction based on current literature. RV contraction consists of three main types: longitudinal shortening, radial shortening, and contraction of LV septum. In contrast to the left ventricle, twisting and rotation motion of the RV are less consistently documented and appear to be less relevant for RV contraction and stroke volume. Longitudinal shortening is due to the longitudinal fibers located on the subendocardial layer and draws the tricuspid and pulmonary valve planes toward the apex. The longitudinal shortening appears to be a major contributor of RV stroke

volume, accounting for approximately 75% of right ventricular stroke volume (Fig. 6.19a). The radial shortening consists of the inward movement of the free wall of RV, mainly due to shortening of subepicardial fibers (Fig. 6.19b). Importantly, the interventricular septum contributes to RV contraction (the systolic interdependence). The contraction of LV, in fact, produces a bulging of the interventricular septum into the RV and simultaneously stretches the free wall of the RV over the septum; both mechanisms thus promote the inward motion of the RV wall, contributing to the reduction of the RV cavity (Fig. 6.19b).

As mentioned, the RV ventricle may be divided into inlet, apical, and outlet. These parts are completely integrated with each other, and many observers consider the RV as a single

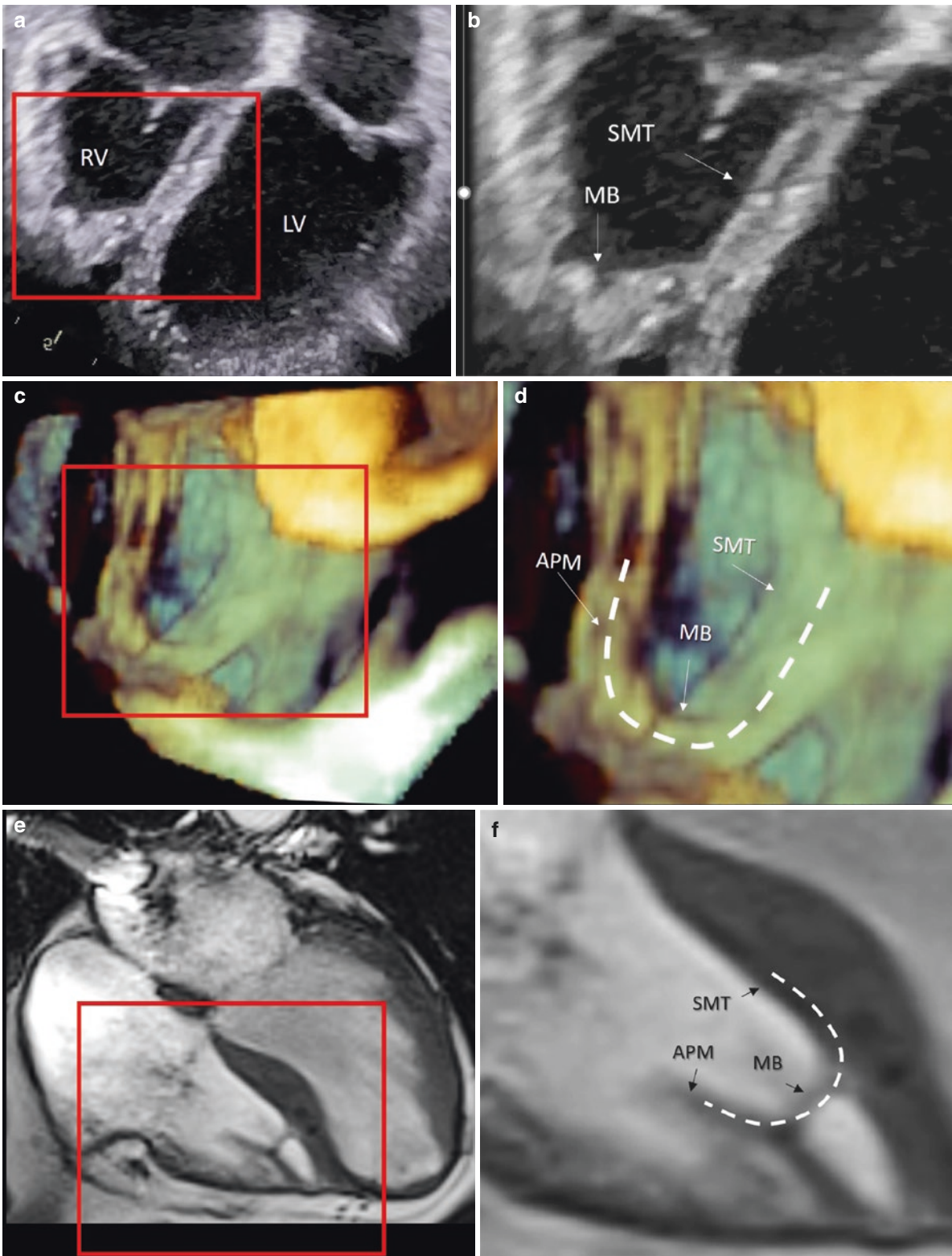


Fig. 6.18 (a) 2D transthoracic echocardiography four-chamber view. The area into the red box is magnified in (b). Images show the septo-marginal trabecula (SMT) in continuity with the moderator band. (c) 3D TEE showing the RV cavity. The area in the red box is magnified in (d). 3D images clearly show the continuity between the SMT, MB, and

anterior papillary muscle (APM). (e) CMR four-chamber view. The area in the red box is magnified in (f). This complex forms a “U-shaped” entity (curved dotted line), that separates the inflow from the outflow (see text)

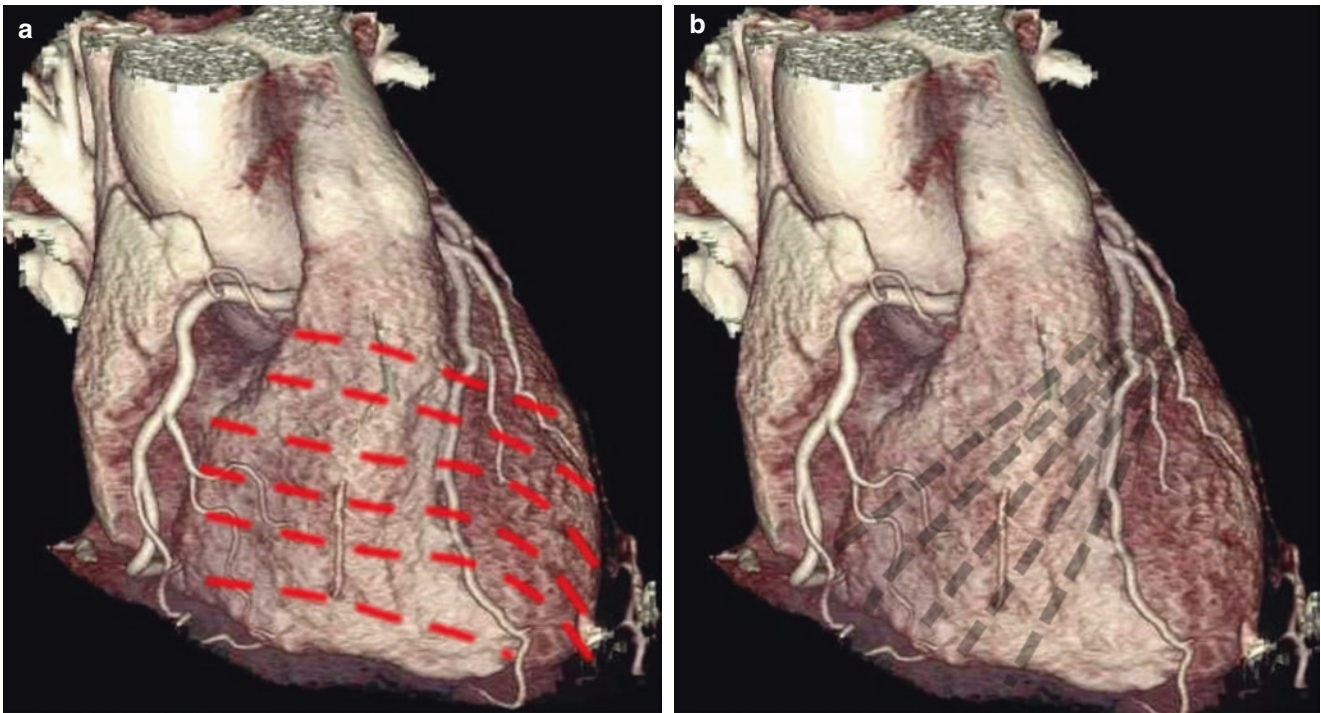


Fig. 6.19 (a) CT volume-rendering images showing the RV fibers of subepicardial layer (*red thick dotted line*) and the RV fibers of subendocardial layer (*b*, black dotted line) (see text)

functional unit. However, the inlet and outlet components may also be considered as distinct chambers given their different embryological origins. Moreover, activation of the outlet occurs relatively late in systole, being the last component of RV to be activated. Thus, regional differences in the time of contraction may be expected. Indeed, a “peristalsis-like” motion theory postulates that the RV inlet contractions occurs 20–40 ms before the RV outflow contraction. This characteristic pattern allows a coordinated movement of the column of flow from the inlet to the outlet, with the blood moving toward the RV outflow a few milliseconds before it contracts. In several reports this peristalsis was documented in cross-sections but not in longitudinal sections. RV focal systolic outpouching in the apical-lateral wall of the RV is rather common in normal subjects and is closely associated with moderator band insertions. This regional wall motion “abnormality,” when occurring in isolation, should be considered a common variant of normal RV pattern of contraction.

The Pulmonary Root

Often the term “pulmonary valve” implies the pulmonary leaflets only (i.e., the thin leaves of connective/elastic tissue that open and close, following the pressure gradient between pulmonary artery and RV). In this chapter we use the term “pulmonary root” for the whole proximal segment of the pul-

monary trunk and its adjoining immediate RV outlet that supports the valvular leaflets. In fact, the pulmonary root comprises the sinotubular junction, the pulmonary sinuses, leaflets, interleaflet triangles, and the ventriculoarterial junction (see below).

2D TTE is the primary imaging technique for the assessment of the normal and abnormal anatomy of the pulmonary valve. However, given its retrosternal location and the tomographic nature of the 2DTTE, simultaneously visualizing the three pulmonary leaflets is very difficult, if not impossible. Also, 2D TEE is not the ideal modality because the PV is the most anterior valve, and therefore the most distant valve from the esophagus. 3D TEE may have the potential to visualize the three pulmonary leaflets from an “en face” perspective. However, the thinness of the leaflets and their position almost parallel to the ultrasound beam combine to produce large dropout artifacts that do not allow acquisition of images of the leaflets in their entirety in “en face” perspective, unlike for aortic leaflets, where dropout artifacts are less pronounced (*see Chap. 2*).

CMR may visualize pulmonary leaflets, but their rapid motion and thinness cause blurring artifacts that reduce the quality of CMR images (*Fig. 6.20*).

CT is able to visualize pulmonary leaflets and its high spatial resolution produces the clearest images of the valve. Unfortunately, its temporal resolution is at best 15 images per second using retrospective imaging acquisition, which is not ideal for appreciating the rapid motion of leaflets.

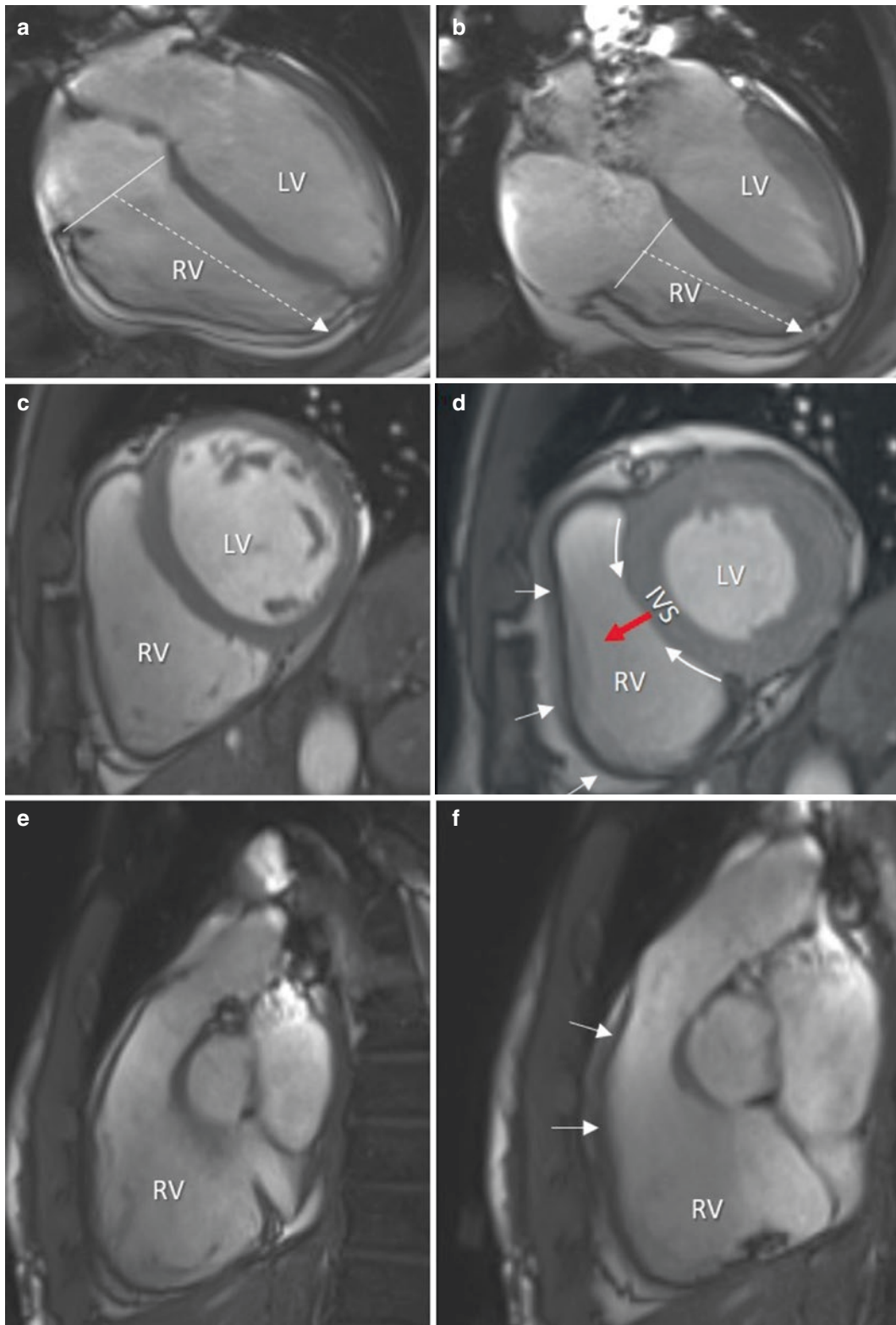


Fig. 6.20 CMR images in four-chamber (**a** and **b**), short-axis view (**c** and **d**) and long-axis views (**e** and **f**), showing the different patterns of contraction of right ventricle (RV). The longitudinal shortening is best appreciated in four-chamber view. The white line indicates the tricuspid annular plane, while the arrow indicates the excursion of the plane towards the apex showing the amount of longitudinal shortening. The

radial shortening is better appreciated in short axis view (**c**, **d**). The small arrows indicate the inward motion of the free lateral wall. The red arrow indicates the bulging of interventricular septum (IVS) and the curved arrows indicate the contraction which stretches the free RV wall, contributing to this inward motion. (**e** and **f**) The inward motion of RV outlet (arrows). LV left ventricle

Moreover, retrospective acquisition causes a significant increase in radiation exposure. Thus, none of the noninvasive imaging techniques is the ideal technique for obtaining consistently good images of pulmonary leaflets. Nevertheless, CT volume-rendering modality may produce exquisite images of the shape of the pulmonary root and inter-leaflet triangles, especially when the acquisition is taken when the contrast is still in the RV cavity, whereas in patients with a favorable transesophageal echocardiographic window, the relatively high spatial (1 mm) and temporal (50 frame/s) resolution permit clear images of pulmonary leaflets for appreciating their motion.

Anatomy

Despite the different pressures, the anatomy of the pulmonary root is almost identical to the aortic root. Indeed, as in the aortic root, it comprises three leaflets, three sinuses of Valsalva, a crown-shaped annulus, commissures, and inter-leaflet fibrous triangles. The pulmonary root is the terminal part of the right ventricular outflow tract and supports pulmonary leaflets. Because in the normal individual the hemodynamic forces in the pulmonary circulation are nearly one fifth of that of systemic circulation, generally, all the components of the pulmonary root are thinner and more delicate and flexible than the aortic counterpart. The *sinu-tubular junction* delimits the pulmonary root from the tubular pulmonary trunk. This junction is not as well-defined as in the left counterpart: a true circular ridge is rarely found—more often it is possible to discern only a line separating the

slightly thinner wall of the sinuses from the thicker wall of the pulmonary trunk.

The *pulmonary leaflets* have the same “bird’s nest” shape as the aortic leaflets, and analogous to the architecture of the aortic leaflets, have a crown-shaped insertion (hingeline) that crosses the ventriculo-arterial junction on the pulmonary wall. Their cranial points, the commissures, reach the sinu-tubular junction, while the most caudal points, the nadirs, are inserted into musculature of the infundibulum. Two leaflets face the right and left aortic leaflets and take the name of right and left leaflets. The third leaflet (the non-facing leaflet), being the most anterior, usually takes the name of anterior leaflet.

The *ventriculo-arterial junction* is the border between the fibro-elastic wall of the vessel (including its sinuses) and the muscular tissue of the infundibulum. Three *interleaflet triangles* arise from the ventriculo-arterial junction up to the sinutubular junction. These triangles are segments of fibrous tissue between the hingelines of adjacent leaflets. Although located at the base of the pulmonary trunk, they are incorporated in the RV when the valve leaflets are in closed position. Interestingly, the nadirs of the pulmonary leaflets cross the ventriculo-arterial junction. In other words, the pulmonary sinuses consist of, distally, the fibro-elastic tissue of arterial wall, and proximally, RV myocardium (Fig. 6.21). Thus, small segments of muscular RV outflow tract are enclosed within the three pulmonary sinuses. These may be sites of arrhythmogenic foci requiring ablation within the sinuses.

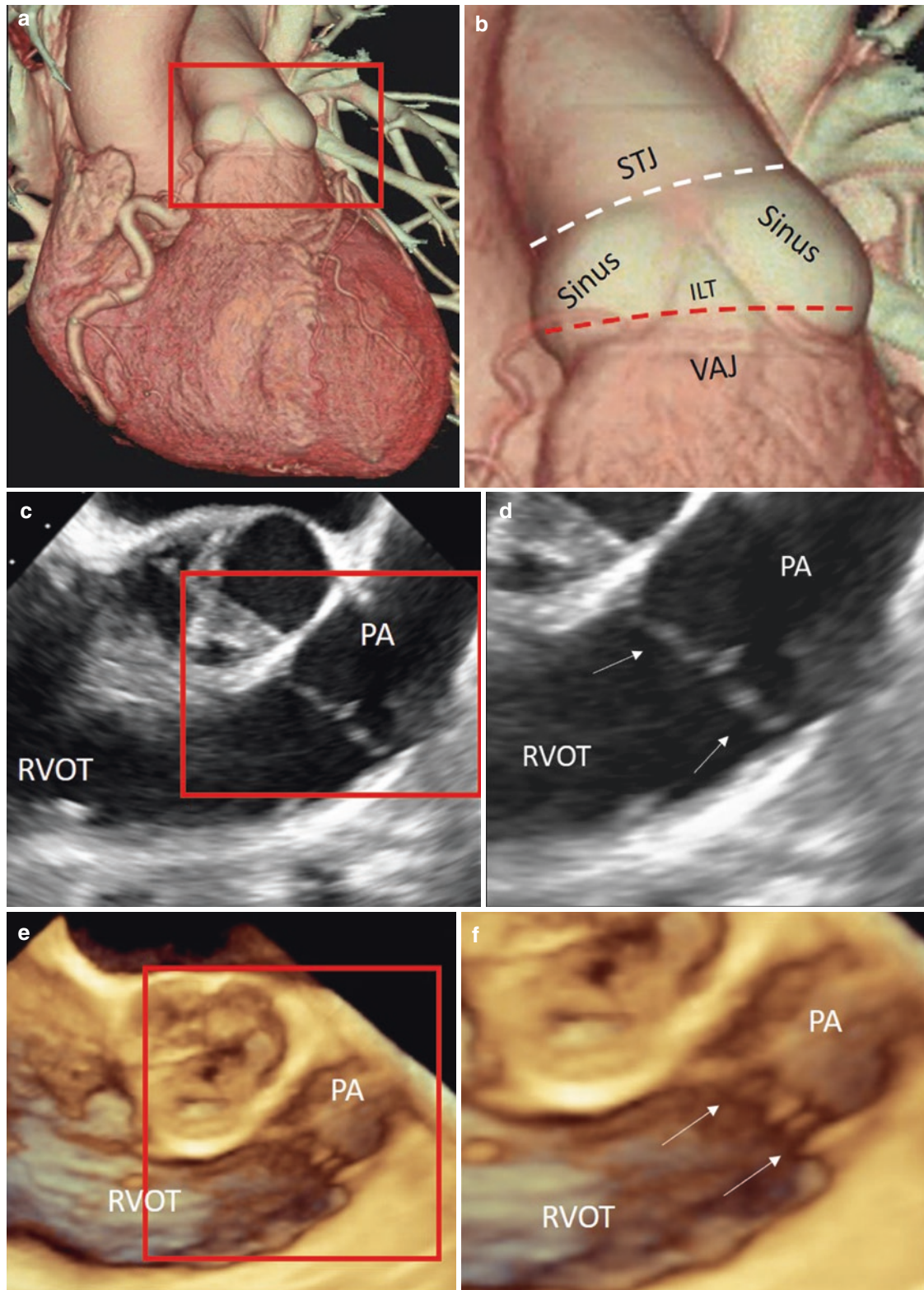


Fig. 6.21 (a) CT image volume-rendering format. The area within the red box is magnified in (b). The magnified image clearly shows the sinu-tubular junction (STJ), marked by a white dotted line, the interleaflet triangle (ILT), and the ventriculo-arterial junction (VAJ) marked with a red dotted line. (c) 2D transesophageal echocardiography in

long-axis view of the right ventricular outflow tract (RVOT). The area within the red box is magnified in (d). Images clearly show the pulmonary leaflets (*arrows*). (e) Same images as in (c) in 3D format. The area within the red box is magnified in (f). *Arrows* indicate pulmonary leaflets. *PA* pulmonary artery

Suggested Reading

- Epstein FH. MRI of left ventricular function. *J Nucl Cardiol.* 2007;14(5):729–44.
- Fernandez-Teran MA, Hrube JM. Myocardial fiber architecture of the human heart. *Anat Rec.* 1982;204:137–47.
- Ho SY. Anatomy and myoarchitecture of the left ventricular wall in normal and in disease. *Eur J Echocardiogr.* 2009;10:i3–7.
- Ho SY, Nihoyannopoulos P. Anatomy, echocardiography, and normal right ventricular dimensions. *Heart.* 2006;92(Suppl I):i2–13.
- Maffei E, Messalli G, Martini C, et al. Left and right ventricle assessment with cardiac CT: validation study vs. cardiac MR. *Eur Radiol.* 2012;22(5):1041–9.
- Sheehan F, Redington A. The right ventricle: anatomy, physiology and clinical imaging. *Heart.* 2008;94:1510–5.
- Stamm C, Anderson RH, Ho SY. Clinical anatomy of the normal pulmonary root compared with that in isolated pulmonary valve stenosis. *J Am Coll Cardiol.* 1998;31(6):1420–5.